

# Model-QED-operator approach to relativistic calculations of the nuclear recoil effect in many-electron atoms and ions

I. S. Anisimova,<sup>1</sup> A. V. Malyshev,<sup>1</sup> D. A. Glazov,<sup>1</sup> M. Y. Kaygorodov,<sup>1</sup>  
Y. S. Kozhedub,<sup>1</sup> G. Plunien,<sup>2</sup> and V. M. Shabaev<sup>1</sup>

<sup>1</sup>*Department of Physics, St. Petersburg State University,  
Universitetskaya 7/9, 199034 St. Petersburg, Russia*

<sup>2</sup>*Institut für Theoretische Physik, Technische Universität Dresden,  
Mommensenstraße 13, D-01062 Dresden, Germany*

## Abstract

A model-operator approach to fully relativistic calculations of the nuclear recoil effect on energy levels in many-electron atomic systems is worked out. The one-electron part of the model operator for treating the normal mass shift beyond the Breit approximation is represented by a sum of semilocal and nonlocal potentials. The latter ones are constructed by employing the diagonal and off-diagonal matrix elements rigorously evaluated for hydrogenlike ions to first order in the electron-to-nucleus mass ratio. The specific mass shift beyond the lowest-order relativistic approximation has a form which can be directly employed in calculations. The capabilities of the method are probed by comparison of its predictions with the results of *ab initio* QED calculations. The proposed operator can be easily incorporated into any relativistic calculation based on the Dirac-Coulomb-Breit Hamiltonian.

## I. INTRODUCTION

An accurate description of the nuclear recoil effect is substantial for the proper analysis of a large number of spectroscopic experiments aimed to measure various atomic properties such as, e.g., binding and transition energies or bound-electron  $g$  factors. Obviously, this effect is most pronounced in isotope differences of the corresponding properties, see, e.g. Refs. [1–11]. The nuclear recoil leads to the so-called mass shift. Along with the field shift caused by the finite-nuclear size, these effects constitute the dominant contribution to the isotope shifts. Joint high-precision theoretical and experimental studies of the isotope differences not only allow one to determine nuclear parameters, e.g., changes in the mean-square charge radii, but also pave the way in the search of new physics [12–22].

Within the  $(m/M)(\alpha Z)^4 mc^2$  approximation, where  $m$  and  $M$  are the masses of the electron and nucleus, respectively,  $\alpha$  is the fine-structure constant, and  $Z$  is the nuclear charge number, the nuclear recoil effect on binding energies can be described by the relativistic mass-shift operator [23–26]. The fully relativistic theory of the nuclear recoil effect to first order in  $m/M$ , to all orders in  $\alpha Z$ , and to zeroth order in  $\alpha$  can be formulated only within the framework of quantum electrodynamics (QED) [23, 24, 26], see also Refs. [27–29]. Despite the smallness of the nuclear-strength parameter  $\alpha Z$  for light atoms, the contribution of the higher orders may nevertheless be significant even in the case of hydrogen [30, 31]. Therefore, an accurate treatment of the nuclear recoil effect demands a nonperturbative (in  $\alpha Z$ ) consideration. To date, the corresponding *ab initio* QED calculations have been performed only for few-electron systems, see, e.g. Refs. [4, 29, 32–34] and references therein. The computational difficulty of the rigorous methods rapidly increases with the number of electrons, which makes them practically infeasible at larger scales. A similar problem exists for evaluation of the radiative QED corrections associated with the electron self-energy and vacuum polarization. For this reason, approximate and efficient approaches for including both the QED and recoil effects within the methods based on the Dirac-Coulomb-Breit Hamiltonian [35–45] are urgent.

For the case of the radiative QED corrections, our group suggested the model-QED-operator approach [46] which recently has been extended to the region of superheavy elements [47]. The QEDMOD Fortran package to generate the operator was presented in Ref. [48]. This operator was successfully applied to the approximate description of the QED effects

on binding and transition energies in various many-electron systems [49–60]. The main goal of the present work is to design a similar approach for the QED calculations of the nuclear recoil effect on energy levels beyond the approximation corresponding to the mass-shift operator. The application of the proposed approach in combination with the standard electron-correlation methods should make possible the approximate QED treatment of this effect in systems where rigorous calculations are rather problematic at the moment.

In view of the significant progress achieved over the past decades in the accuracy of  $g$ -factor measurements in Penning traps [6, 9, 61–67], high-precision evaluation of the nuclear recoil effect in the presence of an external magnetic field becomes essential as well. The QED theory of the nuclear recoil effect on the atomic  $g$  factor valid to all orders in  $\alpha Z$  was elaborated in Ref. [68]. The corresponding *ab initio* calculations have been performed for few-electron ions in Refs. [6, 69–75]. In the case of more complicated systems, the nuclear recoil effect on the bound-electron  $g$  factor can be treated nowadays only within the lowest-order relativistic approximation by means of the effective four-component approach derived from the QED formalism in Ref. [70]. In this context, the model-operator approach developed in the present work for the nuclear recoil effect on binding energies can be considered as a first step towards the construction of a more general operator suitable for studying the bound-electron  $g$  factors as well.

The paper is organized as follows. In Sec. II, we give a brief description of the relativistic theory of the nuclear recoil effect on energy levels in atoms and ions. Sec. III is devoted to the construction of the model operator for QED calculations of the nuclear recoil effect. In Sec. IV, the numerical results are presented in a wide range of  $Z = 5 - 100$ , and the performance of the suggested approach is demonstrated by comparing its predictions with the results of *ab initio* calculations. The nonperturbative (in  $\alpha Z$ ) expressions for the one- and two-electron matrix elements, which describe the nuclear recoil effect on the binding energies, are derived in Appendix A. In Appendix B, these expressions are additionally transformed to make them convenient for practical calculations. Finally, Appendix C summarizes formulas necessary for the construction of the local effective potentials employed in the tests of the model-QED operator in Sec. IV.

Relativistic units ( $\hbar = 1$  and  $c = 1$ ) and the Heaviside charge unit ( $e^2 = 4\pi\alpha$ , where  $e < 0$  is the electron charge) are used throughout the paper.

## II. QED THEORY OF THE NUCLEAR RECOIL EFFECT

As is well known, within the nonrelativistic approximation the nuclear recoil contribution to the binding energy of a hydrogenlike atom can be found by replacing the electron mass  $m$  with the reduced mass,  $m_r = mM/(m + M)$ . For atoms with more than one electron, this recipe is insufficient, and the two-electron part of the nuclear recoil effect has to be taken into account [76]. The lowest-order relativistic (Breit) correction of first order in  $m/M$  can be obtained by employing the mass-shift Hamiltonian [23–25]. For  $N$ -electron system, this operator reads as

$$H_{\text{MS}} = \frac{1}{2M} \sum_{i,j=1}^N \left[ \mathbf{p}_i \cdot \mathbf{p}_j - \frac{\alpha Z}{r_i} \left( \boldsymbol{\alpha}_i + \frac{(\boldsymbol{\alpha}_i \cdot \mathbf{r}_i)}{r_i^2} \mathbf{r}_i \right) \cdot \mathbf{p}_j \right], \quad (1)$$

where the indices  $i$  and  $j$  enumerate the electrons,  $\mathbf{p} = -i\nabla$  is the momentum operator,  $\mathbf{r}$  is the position vector,  $r = |\mathbf{r}|$ , and  $\boldsymbol{\alpha}$  are the Dirac matrices. The first term in the square brackets in Eq. (1) corresponds to the nonrelativistic nuclear recoil operator, whereas the second term determines the leading relativistic correction.

Following Hughes and Eckart [76], the nuclear recoil contribution to atomic spectra is usually divided into the normal (NMS) and specific (SMS) mass shifts. Accordingly, the Hamiltonian (1) can be represented as a sum

$$H_{\text{MS}} = H_{\text{NMS}} + H_{\text{SMS}}, \quad (2)$$

where the first operator corresponds to the terms  $i = j$  in Eq. (1) and the second one corresponds to  $i \neq j$ . For further discussion, it is useful to rewrite Eq. (1) in the form

$$H_{\text{MS}} = \frac{1}{2M} \sum_{i,j=1}^N \left[ \mathbf{p}_i \cdot \mathbf{p}_j - 2\mathbf{D}_i(0) \cdot \mathbf{p}_j \right] \quad (3)$$

by introducing the vector operator

$$\mathbf{D}(0) = \frac{\alpha Z}{2r} \left( \boldsymbol{\alpha} + \frac{(\boldsymbol{\alpha} \cdot \mathbf{r})}{r^2} \mathbf{r} \right). \quad (4)$$

The mass-shift operator  $H_{\text{MS}}$  yields the nuclear recoil corrections up to the order  $(m/M)(\alpha Z)^4 mc^2$ . This operator is widely used in relativistic calculations of atomic spectra and isotope shifts, where the nuclear recoil effect is particularly significant [4, 15, 41, 54, 77–94].

The fully relativistic theory of the nuclear recoil effect on binding energies can be formulated only within the rigorous QED approach (beyond the Breit approximation). To first

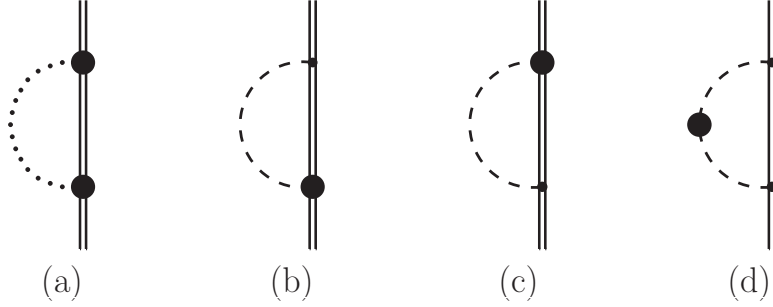


FIG. 1. One-electron nuclear recoil diagrams: the Coulomb (a), one-transverse (b) and (c), and two-transverse (d) contributions. See the text and Ref. [26] for the description of the Feynman rules.

order in  $m/M$ , to all orders in  $\alpha Z$ , and to zeroth order in  $\alpha$  the corresponding theory was developed in Refs. [23, 24, 26]. The formalism worked out in Ref. [26] is the most suitable for the goals of the present study. Within this formalism, the pure nuclear recoil effect is taken into account by modifying the standard QED Hamiltonian of the electron-positron field interacting with the quantized electromagnetic field and the classical Coulomb potential of the nucleus  $V$ . Namely, an extra term is added to the interaction part of the QED Hamiltonian, see Ref. [26] for details. As a result, the pure nuclear recoil effect on energy levels can be obtained on equal footing with the non-recoil QED effects, e.g., the electron self-energy and vacuum polarization, by means of the perturbation theory in the interaction representation of the Furry picture [95]. A convenient approach to construct the QED perturbation series both for single and quasi-degenerate levels is provided by the two-time Green's function (TTGF) method [96]. This method is employed in Appendix A to derive the formal expressions for the matrix elements describing the nuclear recoil effect on binding energies. Within this approach, the zeroth-order one-electron wave functions  $|\psi_n\rangle$  and energies  $\varepsilon_n$  are assumed to be the solutions of the Dirac equation

$$h^D|\psi_n\rangle \equiv [\boldsymbol{\alpha} \cdot \mathbf{p} + \beta m + V]|\psi_n\rangle = \varepsilon_n|\psi_n\rangle. \quad (5)$$

The all-order (in  $\alpha Z$ ) expressions describing the nuclear recoil effect can be divided into the NMS and SMS parts as well. The one-electron (NMS) and two-electron (SMS) contributions are given by the Feynman diagrams shown in Figs. 1 and 2, respectively. The exhaustive description of the additional diagram-technique rules, which arise in connection with the treatment of the nuclear recoil effect, can be found in Ref. [26], see also Ref. [96].

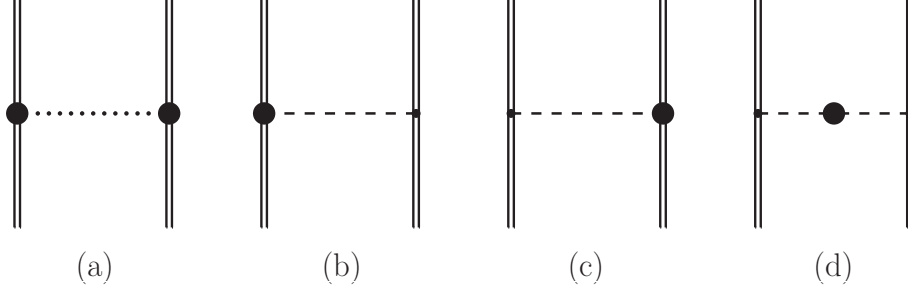


FIG. 2. Two-electron nuclear recoil diagrams: the Coulomb (a), one-transverse (b) and (c), and two-transverse (d) contributions.

To explain the terminology employed throughout the paper, we briefly comment on these rules using Fig. 1 as an example. First of all, the double line and the vertex with a small dot in the figure correspond to the conventional diagram technique of the bound-state QED [96]. Namely, the line denotes the electron propagator in the potential  $V$ , and the vertex arises from the standard interaction of the electron-positron and electromagnetic fields. All the other diagram elements originate due to the presence of the aforementioned extra term in the QED Hamiltonian. The Coulomb gauge established itself as the most appropriate one for the nuclear-recoil-effect studies [23, 24, 26, 28], and it leads to the natural terminology. In this gauge, the photon propagator  $D_{\mu\nu}(\omega, \mathbf{r})$  is divided into the Coulomb,

$$D_{00}(\omega, \mathbf{r}) = \frac{1}{4\pi r}, \quad (6)$$

and transverse,

$$D_{lk}(\omega, \mathbf{r}) = -\frac{1}{4\pi} \left[ \frac{\exp(i\sqrt{\omega^2 + i0} r)}{r} \delta_{lk} + \nabla_l \nabla_k \frac{\exp(i\sqrt{\omega^2 + i0} r) - 1}{\omega^2 r} \right]. \quad (7)$$

parts, while the remaining components of the photon propagator are equal to zero,  $D_{l0} = D_{0l} = 0$  ( $l, k = 1, 2, 3$ ). All the recoil contributions in Fig. 1 can be classified with respect to the number of the propagators (7) involved. There are three possibilities [26]: (i) the dotted line connecting two bold dots in Fig. 1(a) depicts the so-called ‘‘Coulomb recoil’’ interaction, which does not contain the transverse part of the photon propagator at all; (ii) the dashed line with the bold dot at one of the ends in Figs. 1(b) and 1(c) stands for the ‘‘one-transverse-photon recoil’’ interaction, which includes  $D_{lk}$  once; (iii) finally, the dashed line with the bold dot in the middle in Fig. 1(d) designates the ‘‘two-transverse-photon recoil’’ interaction,

which involves the product of two photon propagators. We note that the approach initially developed in Ref. [23] leads to the same result as the formalism of Ref. [26] but it implies the summation of the infinite sequences of Feynman diagrams describing the electron-nucleus interaction via photon exchange. In this case, the three discussed possibilities correspond to the summation of the diagrams with zero, one, and two transverse photons and an arbitrary number of the Coulomb photons.

To all orders in  $\alpha Z$ , the NMS contribution for the state  $|\psi_a\rangle$  can be expressed as follows [23, 26]

$$E_{\text{NMS}} = \langle \psi_a | \mathbf{P}(\varepsilon_a) | \psi_a \rangle, \quad (8)$$

where we have introduced the operator  $\mathbf{P}(E)$  by

$$\langle \psi_i | \mathbf{P}(E) | \psi_k \rangle = \frac{i}{2\pi} \int_{-\infty}^{\infty} d\omega \sum_n \frac{\langle \psi_i \psi_n | R(\omega) | \psi_n \psi_k \rangle}{E - \omega - \varepsilon_n(1 - i0)} \quad (9)$$

with

$$R(\omega) = \frac{1}{M} \left[ \mathbf{p}_1 - \mathbf{D}_1(\omega) \right] \cdot \left[ \mathbf{p}_2 - \mathbf{D}_2(\omega) \right]. \quad (10)$$

In Eq. (9),  $|\psi_i \psi_n\rangle = |\psi_i\rangle |\psi_n\rangle$  is the direct product of the one-electron wave functions. The operator  $\mathbf{D}(\omega)$  in Eq. (10) is related to the transverse part of the photon propagator (7), and its  $k$ th Cartesian component,  $D_k(\omega)$ , is equal to

$$D_k(\omega) = -4\pi\alpha Z\alpha_l D_{lk}(\omega). \quad (11)$$

The  $\omega \rightarrow 0$  limit of the operator  $\mathbf{D}(\omega)$  coincides with formula (4). The indices 1 and 2 in Eq. (10) designate the electron, on which the corresponding operators act. Let us rewrite  $R(\omega)$  in the form:

$$R(\omega) = R_c + R_{\text{tr1}}(\omega) + R_{\text{tr2}}(\omega), \quad (12)$$

$$R_c = \frac{1}{M} \mathbf{p}_1 \cdot \mathbf{p}_2, \quad (13)$$

$$R_{\text{tr1}}(\omega) = -\frac{1}{M} \left[ \mathbf{p}_1 \cdot \mathbf{D}_2(\omega) + \mathbf{D}_1(\omega) \cdot \mathbf{p}_2 \right], \quad (14)$$

$$R_{\text{tr2}}(\omega) = \frac{1}{M} \mathbf{D}_1(\omega) \cdot \mathbf{D}_2(\omega). \quad (15)$$

Substituting Eq. (12) into Eq. (8), one arrives at the Coulomb, one-transverse-photon, and two-transverse-photon contributions to the NMS.

Let us turn to the discussion of the SMS contribution which corresponds to the Feynman diagrams in Fig. 2. For simplicity, we consider the case of a one-determinant unperturbed wave function,

$$\Psi_{ab}(\mathbf{r}_1, \mathbf{r}_2) = \frac{1}{\sqrt{2}} \sum_P (-1)^P \psi_{Pa}(\mathbf{r}_1) \psi_{Pb}(\mathbf{r}_2), \quad (16)$$

where  $P$  is the permutation operator. The generalization to the case of a many-determinant wave function is straightforward. The nonperturbative (in  $\alpha Z$ ) expression for the SMS contribution reads as [24, 26]

$$E_{\text{SMS}} = -\langle \psi_b \psi_a | R(\Delta) | \psi_a \psi_b \rangle, \quad (17)$$

where  $\Delta = \varepsilon_a - \varepsilon_b$ . The formula (17) gives the “exchange” term for the two-electron operator  $R$ . The “direct” one is equal to zero, since the matrix elements of the operators  $\mathbf{p}$  and  $\mathbf{D}$  are zeroes for states of the same parity. Substituting (12) into Eq. (17), one obtains the expansion of the SMS contribution into the Coulomb, one-transverse-photon, and two-transverse-photon parts.

Over the past three decades, numerous QED calculations of the nuclear recoil effect on binding energies were carried out [4, 29, 31–34, 84, 88, 97, 98]. We should note that the expressions (8) and (17) with the operator  $\mathbf{D}$  defined by Eq. (11) are derived for the point-nucleus case. In Ref. [33], it was argued that the dominant part of the finite-nuclear size (FNS) correction to the nuclear recoil effect can be accounted for by employing the potential of the extended nucleus in Eq. (5), and since that paper this prescription is usually used in the QED calculations of the mass shift. It was also found there that the treatment of the FNS correction to the nuclear recoil effect within the Breit approximation defined by the operator (1) leads to an artificial contribution of order  $(m/M)(\alpha Z)^5 (R_{\text{nucl}}/\lambda) mc^2$  which even exceeds the main contribution of order  $(m/M)(\alpha Z)^4 (R_{\text{nucl}}/\lambda)^2 mc^2$  (here  $\lambda = \hbar/(mc)$  is the Compton wavelength). This artificial contribution arises from the first (Coulomb) term in Eq. (1). However, it is completely cancelled by the corresponding FNS correction to the Coulomb part of the QED nuclear recoil effect, which means that the rigorous theory for the FNS contribution beyond the main  $(m/M)(\alpha Z)^4 (R_{\text{nucl}}/\lambda)^2 mc^2$  term can be formulated only within the framework of QED. In Ref. [99], an additional FNS correction, which results from modifying the Breit-approximation mass-shift operator (1) by inserting the form factor into the nuclear vertex [100, 101], was evaluated. This operator differs from the one obtained by considering the zero-frequency limit of the photon propagator in the modified



Coulomb gauge [102, 103]. The main difference between the results obtained using these two operators is due to a spurious contribution of the order  $(m/M)(\alpha Z)^5(R_{\text{nucl}}/\lambda)mc^2$  in the one-transverse-photon part, which occurs only in the calculation with the operator from Ref. [102, 103]. Like to the case of the Coulomb contribution, this spurious term is cancelled by the related FNS contribution to the one-transverse-photon QED correction, provided it is also calculated with the photon propagator in the modified Coulomb gauge [102, 103]. In Refs. [34, 71, 119], the additional FNS correction from Ref. [99], which is free from the spurious term, was used to estimate the uncertainty of the calculations based on the prescription of Ref. [33]. To date, the most elaborated evaluation of the FNS correction to the nuclear recoil effect was performed within the QED approach in Ref. [102]. This calculation accomplished for the  $1s$  state has confirmed that the dominant part of the FNS correction to the nuclear recoil effect is indeed covered by the recipe of Ref. [33], which we also follow here. The rigorous QED treatment of the total FNS correction to the nuclear recoil effect lies beyond the scope of the present work.

Restricting Eqs. (8) and (17) by the lowest-order relativistic approximation leads to the NMS and SMS parts of the MS operator (1), respectively. Until recently, all nonperturbative (in  $\alpha Z$ ) calculations were limited by the zeroth order in  $1/Z$ , i.e., the electron-electron interaction corrections to the nuclear recoil effect were considered at best only within the Breit approximation. In our recent works, we have advanced the QED theory of the nuclear recoil effect. Specifically, we have considered to all orders in  $\alpha Z$  the electron-electron interaction correction of first order in  $1/Z$  to the one-electron [104] and two-electron [105] parts of the nuclear recoil effect on binding energies in atoms and ions. These higher-order QED contributions being also beyond the scope of the present work can be calculated additionally if needed.

Finally, the radiative ( $\sim \alpha$ ) as well as the second-order (in  $m/M$ ) recoil corrections are accessible nowadays only within the  $\alpha Z$ -expansion approaches, see Refs. [106–108] and references therein. These contributions are also not considered in this paper.

### III. MODEL-QED OPERATOR FOR THE NUCLEAR RECOIL EFFECT

The QED calculations for many-electron systems, becoming increasingly relevant in view of the considerable progress of the experiment, are complicated and in many cases currently



FIG. 3. Self-energy diagram.

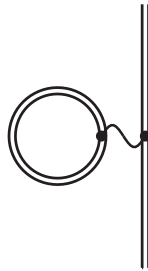


FIG. 4. Vacuum-polarization diagram.

inaccessible. This is true for the radiative corrections as well as for the QED treatment of the nuclear recoil effect. For this reason, there is a vital need for a simple approximate approach for taking into account the QED corrections in various relativistic calculations. The conventional first-order QED corrections correspond to the self-energy (SE), vacuum-polarization (VP), and one-photon-exchange diagrams shown in Figs. 3, 4, and 5, respectively. The approximate model-QED-operator approach to evaluate these effects has been suggested recently by our group in Refs. [46–48]. In this section, the analogy will be traced that allows us

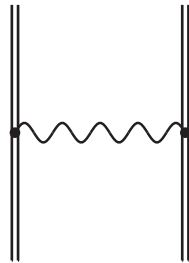


FIG. 5. One-photon exchange diagram.

to construct a similar approach for the nuclear recoil contributions beyond the lowest-order relativistic approximation.

The model-QED-operator approach [46] is worked out within the TTGF method. It is based on the fact that the QED effects to first order in  $\alpha$  can be described by an effective Hamiltonian acting in the subspace which is spanned by all Slater determinants made up of the positive-energy solutions of the Dirac equation (5), see Ref. [109] for details. This effective Hamiltonian has the form

$$H = \Lambda^{(+)} \left[ \sum_i^N (h_i^D + h_i^{\text{SE}} + h_i^{\text{VP}}) + \sum_{i<j}^N h_{ij}^{\text{1ph}} \right] \Lambda^{(+)}, \quad (18)$$

where  $\Lambda^{(+)}$  is the product of the one-electron projectors on the positive-energy eigenfunctions of the Dirac Hamiltonian  $h^D$ , and the operators  $h^{\text{SE}}$ ,  $h^{\text{VP}}$ , and  $h^{\text{1ph}}$  arise from the diagrams in Figs. 3, 4, and 5, respectively. According to the QED theory of the nuclear recoil effect, described briefly in Sec. II, to first order in  $m/M$  and to all orders in  $\alpha Z$ , the Hamiltonian  $H$  has to be supplemented by the term

$$\delta H = \Lambda^{(+)} \left[ \sum_i^N h_i^{\text{NMS}} + \sum_{i<j}^N h_{ij}^{\text{SMS}} \right] \Lambda^{(+)}, \quad (19)$$

where the operators  $h^{\text{NMS}}$  and  $h^{\text{SMS}}$  are associated with the diagrams in Figs. 1 and 2, respectively. Below we discuss how the part of the operator  $\delta H$  which is beyond the Breit approximation can be adapted for the practical relativistic electronic-structure calculations. We note that the entire formalism can be generalized to the case where the potential  $V$  in Eq. (5) along with the nuclear potential includes also some local screening potential  $V_{\text{scr}}$  modeling the interelectronic-interaction effects within the initial approximation, i.e., to the extended version of the Furry picture.

Let us start with the analogy between the one-photon-exchange diagram in Fig. 5 and the two-electron nuclear recoil diagrams in Fig. 2. For the one-photon-exchange diagram, the TTGF method leads to the following symmetric expression [96, 109]

$$h^{\text{1ph}} = \sum_{\substack{\varepsilon_{i_1}, \varepsilon_{i_2}, \varepsilon_{k_1}, \varepsilon_{k_2} > 0 \\ i_1 \neq i_2, k_1 \neq k_2}} |\psi_{i_1} \psi_{i_2}\rangle \langle \psi_{i_1} \psi_{i_2} | \frac{1}{2} \left[ I(\varepsilon_{i_1} - \varepsilon_{k_1}) + I(\varepsilon_{i_2} - \varepsilon_{k_2}) \right] |\psi_{k_1} \psi_{k_2}\rangle \langle \psi_{k_1} \psi_{k_2} |, \quad (20)$$

where the indices  $i_1$ ,  $i_2$ ,  $k_1$ , and  $k_2$  enumerate the positive-energy one-electron Dirac eigenfunctions,

$$I(\omega) = e^2 \alpha_1^\mu \alpha_2^\nu D_{\mu\nu}(\omega, r_{12}), \quad (21)$$

$\alpha^\mu \equiv \gamma^0 \gamma^\mu = (1, \boldsymbol{\alpha})$  are the Dirac matrices, and the photon propagator in the Coulomb gauge is given by Eqs. (6) and (7). The matrix elements for the two-electron nuclear recoil diagrams are derived within the TTGF method in Appendix A, see Eq. (A21) for the final formula. As a result, the operator  $h^{\text{SMS}}$  can be represented as

$$h^{\text{SMS}} = \sum_{\substack{\varepsilon_{i_1}, \varepsilon_{i_2}, \varepsilon_{k_1}, \varepsilon_{k_2} > 0 \\ i_1 \neq i_2, k_1 \neq k_2}} |\psi_{i_1} \psi_{i_2}\rangle \langle \psi_{i_1} \psi_{i_2}| \frac{1}{2} \left[ R(\varepsilon_{i_1} - \varepsilon_{k_1}) + R(\varepsilon_{i_2} - \varepsilon_{k_2}) \right] |\psi_{k_1} \psi_{k_2}\rangle \langle \psi_{k_1} \psi_{k_2}|, \quad (22)$$

where the operator  $R(\omega)$  is defined by Eq. (10). Therefore, the expressions (20) and (22) differ only by the replacement of  $I$  with  $R$ . Taking the photon propagator  $D_{\mu\nu}(\omega, r_{12})$  in the Coulomb gauge at the zero-energy transfer ( $\omega = 0$ ), one obtains from Eq. (20) the interaction part of the Dirac-Coulomb-Breit Hamiltonian. In the Coulomb gauge, the formula (20) considered beyond the lowest-order relativistic approximation leads to the so-called frequency-dependent Breit interaction. The corresponding correction is readily taken into account within the electronic-structure calculations, see, e.g., Refs. [57, 60, 110–113], and does not require the construction of the model operator. When omitting the two-transverse-photon contribution and taking the  $\omega \rightarrow 0$  limit in  $R(\omega)$ , the expression (22) boils down to the SMS part of the mass-shift operator (1). The remaining part of the contribution given by Eq. (22) can be treated on equal footing with the frequency-dependent Breit-interaction correction.

Now we turn to the discussion of the one-electron contributions. The VP diagram in Fig. 4 does not have a counterpart in the QED theory of the nuclear recoil effect. Therefore, we will focus on the SE diagram in Fig. 3 and the one-electron nuclear recoil diagrams in Fig. 1. First, let us introduce the SE operator  $\Sigma(E)$ ,

$$\langle \psi_i | \Sigma(E) | \psi_k \rangle = \frac{i}{2\pi} \int_{-\infty}^{\infty} d\omega \sum_n \frac{\langle \psi_i \psi_n | I(\omega) | \psi_n \psi_k \rangle}{E - \omega - \varepsilon_n(1 - i0)}. \quad (23)$$

This formal expression suffers from ultraviolet divergences and has to be renormalized together with the mass counterterm, see, e.g., Refs. [114–117]. Within the TTGF method, one can obtain the following symmetric expression for the operator  $h^{\text{SE}}$  [46, 109]:

$$h^{\text{SE}} = \sum_{i,k}^{\varepsilon_i, \varepsilon_k > 0} |\psi_i\rangle \langle \psi_i| \frac{1}{2} \left[ \Sigma_R(\varepsilon_i) + \Sigma_R(\varepsilon_k) \right] |\psi_k\rangle \langle \psi_k|, \quad (24)$$

where  $\Sigma_R(\varepsilon)$  is the renormalized SE operator. The corresponding diagonal and off-diagonal matrix elements are tabulated, e.g., in Refs. [46, 47]. The matrix elements for the one-electron nuclear recoil diagrams are considered in the framework of the TTGF method in

Appendix A, see Eq. (A14) for the final expression. In contrast to the SE diagram, this contribution is ultraviolet finite and does not require any regularization. Nevertheless, its evaluation is a complex task compared to the calculations with the mass-shift Hamiltonian (1). The operator  $h^{\text{NMS}}$  valid to all orders in  $\alpha Z$  can be written in the form

$$h^{\text{NMS}} = \sum_{i,k}^{\varepsilon_i, \varepsilon_k > 0} |\psi_i\rangle\langle\psi_i| \frac{1}{2} \left[ P(\varepsilon_i) + P(\varepsilon_k) \right] |\psi_k\rangle\langle\psi_k|, \quad (25)$$

The analogy between Eqs. (24) and (25) is evident, and it is employed in the present work to develop the model-QED-operator approach for the one-electron nuclear recoil contribution. Since within the Breit approximation this contribution can be treated by means of the operator

$$h_{\text{Breit}}^{\text{NMS}} = \frac{1}{2M} [\mathbf{p}^2 - 2\mathbf{D}(0) \cdot \mathbf{p}], \quad (26)$$

we construct the model operator for the remaining (QED) part of  $h^{\text{NMS}}$ , namely for

$$h_{\text{h.o.}}^{\text{NMS}} \equiv \sum_{i,k}^{\varepsilon_i, \varepsilon_k > 0} |\psi_i\rangle\langle\psi_i| \left\{ \frac{1}{2} [P(\varepsilon_i) + P(\varepsilon_k)] - h_{\text{Breit}}^{\text{NMS}} \right\} |\psi_k\rangle\langle\psi_k|. \quad (27)$$

The model-operator approach should simultaneously solve two issues. First, since there is no simple-enough procedure for the *ab initio* evaluation of the P-operator matrix elements for arbitrary levels (including the continuum-spectrum levels), one has to terminate the summation in Eq. (27). Second, the short interaction range should be kept. To address these problems, similarly to Ref. [46], we approximate the QED recoil operator  $h_{\text{h.o.}}^{\text{NMS}}$  by a sum of semilocal (with respect to  $r$ ) and nonlocal potentials

$$\tilde{h}_{\text{h.o.}}^{\text{NMS}} = V_{\text{s.l.}} + V_{\text{n.l.}}. \quad (28)$$

The operator P, like the operator  $\Sigma_R$ , conserves the relativistic angular quantum number  $\kappa = (-1)^{j+l+1/2}(j+1/2)$ , where  $j$  and  $l$  are the total and orbital angular momenta, respectively. For this reason, the semilocal potential can be written as

$$V_{\text{s.l.}} = \sum_{\kappa} V_{\text{s.l.}}^{\kappa} P_{\kappa}, \quad (29)$$

where the projector  $P_{\kappa}$  acts only on the angular variables, and its kernel is

$$P_{\kappa}(\mathbf{n}, \mathbf{n}') = \begin{pmatrix} \sum_m \Omega_{\kappa m}(\mathbf{n}) \Omega_{\kappa m}^{\dagger}(\mathbf{n}') & 0 \\ 0 & \sum_m \Omega_{-\kappa m}(\mathbf{n}) \Omega_{-\kappa m}^{\dagger}(\mathbf{n}') \end{pmatrix} \quad (30)$$

with  $\Omega_{\kappa m}(\mathbf{n})$  being the spherical spinor and  $\mathbf{n} = \mathbf{r}/r$ . In Eq. (29), we take

$$V_{\text{s.l.}}^{\kappa}(r) = A_{\kappa} \exp(-r/\lambda), \quad (31)$$

where the parameters  $A_{\kappa}$  are chosen to reproduce the *ab initio* values of the diagonal matrix elements of the operator  $h_{\text{h.o.}}^{\text{NMS}}$  for the state with the lowest principal quantum number  $n$  for a given  $\kappa$ . The nonlocal potential can be written in the form

$$V_{\text{n.l.}} = \sum_{j,l=1}^n |\phi_j\rangle B_{jl} \langle \phi_l|, \quad (32)$$

where the functions  $\{\phi_i\}_{i=1}^n$ , as in Ref. [46], are chosen to be

$$\phi_i(\mathbf{r}) = \frac{1}{2} [I - (-1)^{s_i} \beta] \rho_{l_i}(r) \psi_i(\mathbf{r}). \quad (33)$$

Here the index  $s_i = n_i - l_i$  enumerates the positive-energy states for the given angular symmetry,  $I$  and  $\beta$  are the identity and the standard Dirac matrices, respectively, and the factors  $\rho_{l_i}(r) = \exp[-2\alpha Z(r/\lambda)/(1+l_i)]$  provide the stronger localization of the functions  $\{\phi_i\}_{i=1}^n$  as compared to the eigenfunctions  $\{\psi_i\}_{i=1}^n$  of the Dirac equation (5). Finally, the coefficients  $B_{jl}$  in Eq. (32) are determined from the condition that the matrix elements of the model-QED operator  $\tilde{h}_{\text{h.o.}}^{\text{NMS}}$  evaluated in the space spanned by the functions  $\{\psi_i\}_{i=1}^n$  coincide with the exact ones. This leads to the following equations

$$\sum_{j,l}^n \langle \psi_i | \phi_j \rangle B_{jl} \langle \phi_l | \psi_k \rangle = \langle \psi_i | \left\{ \frac{1}{2} [P(\varepsilon_i) + P(\varepsilon_k)] - h_{\text{Breit}}^{\text{NMS}} - V_{\text{s.l.}} \right\} | \psi_k \rangle \quad (34)$$

for  $i, k = 1 \dots n$ , see Ref. [46] for details. We note that the model-QED operator for the nuclear recoil effect is worked out in such a way that the QEDMOD Fortran package [48] can be readily adapted to incorporate it. We propose to refer to the resulting package as the RECMOD one.

Therefore, to determine the model-QED operator we need to calculate the diagonal and off-diagonal matrix elements of the QED recoil operator  $h_{\text{h.o.}}^{\text{NMS}}$  with the Dirac-Coulomb wave functions. So far, only calculations of the diagonal matrix elements have been presented in the literature. In this work, the expressions derived within the TTGF method are employed for the *ab initio* QED evaluation of the one-electron nuclear recoil contributions. Concluding the description of the model-QED operator, we note that in practical calculations we construct the model operator employing the functions (33) which correspond to the  $ns$  states with the principal quantum number  $n \leq 3$  and the  $np_{1/2}$ ,  $np_{3/2}$ ,  $nd_{3/2}$ , and  $nd_{5/2}$  states with  $n \leq 4$ .

#### IV. TEST OF THE MODEL-QED OPERATOR FOR THE NUCLEAR RECOIL EFFECT

In the present work, to obtain the diagonal and off-diagonal matrix elements of the higher-order operator  $h_{\text{h.o.}}^{\text{NMS}}$ , we first evaluate the corresponding values for the operator  $h^{\text{NMS}}$  and then numerically subtract the Breit contribution given by the operator  $h_{\text{Breit}}^{\text{NMS}}$ . For the Coulomb part of the nuclear recoil effect, this subtraction is readily accomplished analytically by omitting the summation over the positive-energy states and doubling the contribution of the negative-energy continuum in Eq. (B2). This can be useful to avoid large cancellations for low values of  $Z$ . The calculations are performed for the  $ns$ ,  $np_{1/2}$ ,  $np_{3/2}$ ,  $nd_{3/2}$ , and  $nd_{5/2}$  states with the principal quantum number  $n \leq 5$  in the wide range of  $Z = 5 - 100$  using the Dirac-Coulomb wave functions. The evaluation is carried out for the potential of the extended nucleus in Eq. (5). The nuclear-charge distribution is described by the homogeneously-charged-sphere model for  $Z \leq 14$ , and by the Fermi model otherwise. The nuclear-charge radii are taken from Refs. [118, 119]. The one-electron basis set to represent the electron Green's function is constructed from B splines [120] within the dual-kinetic-balance approach [121]. The  $\omega$  integration is performed in accordance with the equations presented in Appendix B.

The results of the *ab initio* calculations are conveniently expressed in terms of the dimensionless function  $F_{n_i n_k}(\alpha Z)$  defined by

$$\langle \psi_i | h_{\text{h.o.}}^{\text{NMS}} | \psi_k \rangle = \frac{m}{M} \frac{(\alpha Z)^5}{(n_i n_k)^{3/2}} F_{n_i n_k}(\alpha Z) m c^2. \quad (35)$$

Our data for the  $ns$ ,  $np_{1/2}$ ,  $np_{3/2}$ ,  $nd_{3/2}$ , and  $nd_{5/2}$  states are presented in Tables I, II, III, IV, and V, respectively. The individual Coulomb, one- and two-transverse-photon corrections as well as the total QED recoil contributions are shown. The uncertainties due to the approximate treatment of the nuclear-size correction are omitted, and with this in mind the values are accurate to all digits quoted. The function  $F_{n_i n_k}(\alpha Z)$  for values of  $Z$  not listed in Tables I-V can be obtained using a polynomial fitting,

$$F_{n_i n_k}(\alpha Z) = \sum_{n=1}^N F_{n_i n_k}(\alpha Z_n) \prod_{m \neq n} \frac{Z - Z_m}{Z_n - Z_m}. \quad (36)$$

The model-QED operator for the nuclear recoil effect is constructed using the matrix elements for the  $ns$  states with  $n \leq 3$  and the  $np$  and  $nd$  states with  $n \leq 4$ . By definition,

TABLE I. Matrix elements of the operator  $h_{\text{h.o.}}^{\text{NMS}}$  for the  $ns$  states calculated with the Dirac-Coulomb wave functions for the extended nuclei. Labels ( $n_i, n_k$ ) stand for the function  $F_{n_i n_k}$  defined by Eq. (35). Rows labeled “c”, “tr1”, “tr2”, and “tot” contain the Coulomb, one-transverse-photon, two-transverse-photon and total nuclear recoil contributions, respectively.

Z	Term	(1,1)	(1,2)	(1,3)	(1,4)	(1,5)	(2,2)	(2,3)	(2,4)	(2,5)	(3,3)	(3,4)	(3,5)	(4,4)	(4,5)	(5,5)
5	c	-0.38522	-0.38532	-0.38531	-0.38530	-0.38528	-0.38542	-0.38540	-0.38539	-0.38538	-0.38539	-0.38538	-0.38537	-0.38537	-0.38536	-0.38535
	tr1	2.73291	2.80247	2.80794	2.80923	2.80968	2.92571	2.94192	2.94448	2.94525	2.97187	2.97825	2.97968	2.98997	2.99314	2.99890
	tr2	-0.97002	-0.93991	-0.93526	-0.93365	-0.93291	-0.93021	-0.92415	-0.92237	-0.92156	-0.92221	-0.92003	-0.91917	-0.91932	-0.91830	-0.91796
	tot	1.37767	1.47725	1.48737	1.49028	1.49149	1.61008	1.63236	1.63672	1.63831	1.66426	1.67284	1.67514	1.68528	1.68949	1.69560
10	c	-0.35934	-0.35973	-0.35970	-0.35965	-0.35961	-0.36014	-0.36010	-0.36006	-0.36002	-0.36007	-0.36002	-0.35999	-0.35998	-0.35994	-0.35990
	tr1	2.22748	2.29820	2.30346	2.30451	2.30478	2.42164	2.43753	2.43983	2.44040	2.46708	2.47317	2.47439	2.48457	2.48752	2.49305
	tr2	-0.65044	-0.61934	-0.61459	-0.61292	-0.61213	-0.60724	-0.60083	-0.59894	-0.59808	-0.59833	-0.59599	-0.59506	-0.59505	-0.59393	-0.59347
	tot	1.21770	1.31912	1.32916	1.33194	1.33304	1.45427	1.47660	1.48083	1.48230	1.50867	1.51716	1.51935	1.52954	1.53365	1.53968
15	c	-0.34002	-0.34033	-0.34087	-0.34078	-0.34070	-0.34186	-0.34180	-0.34171	-0.34163	-0.34175	-0.34165	-0.34157	-0.34155	-0.34147	-0.34139
	tr1	1.95262	2.02557	2.03060	2.03134	2.03137	2.15064	2.16624	2.16819	2.16849	2.19543	2.20116	2.20211	2.21217	2.21484	2.22007
	tr2	-0.48917	-0.45702	-0.45212	-0.45037	-0.44953	-0.44251	-0.43573	-0.43374	-0.43281	-0.43267	-0.43016	-0.42916	-0.42898	-0.42777	-0.42718
	tot	1.12343	1.22761	1.23760	1.24019	1.24115	1.36627	1.38870	1.39275	1.39405	1.42101	1.42936	1.43139	1.44163	1.44560	1.45149
20	c	-0.32433	-0.32595	-0.32587	-0.32570	-0.32557	-0.32763	-0.32754	-0.32738	-0.32725	-0.32746	-0.32710	-0.32717	-0.32714	-0.32701	-0.32687
	tr1	1.77226	1.84842	1.85320	1.85357	1.85329	1.97645	1.99178	1.99333	1.99329	2.02067	2.02599	2.02661	2.03655	2.03887	2.04373
	tr2	-0.38809	-0.35477	-0.34970	-0.34785	-0.34695	-0.33781	-0.33063	-0.32852	-0.32752	-0.32701	-0.32432	-0.32324	-0.32291	-0.32160	-0.32089
	tot	1.05985	1.16769	1.17764	1.18001	1.18077	1.31101	1.33361	1.33743	1.33852	1.36621	1.37437	1.37620	1.38649	1.39027	1.39597
25	c	-0.31216	-0.31472	-0.31460	-0.31436	-0.31416	-0.31736	-0.31725	-0.31702	-0.31681	-0.31715	-0.31691	-0.31671	-0.31668	-0.31647	-0.31627
	tr1	1.64447	1.72480	1.72933	1.72925	1.72860	1.85711	1.87222	1.87330	1.87286	1.90087	1.90570	1.90593	1.91576	1.91768	1.92211
	tr2	-0.31779	-0.28313	-0.27786	-0.27591	-0.27495	-0.26362	-0.25602	-0.25379	-0.25273	-0.25183	-0.24896	-0.24782	-0.24733	-0.24593	-0.24511
	tot	1.01453	1.12695	1.13687	1.13898	1.13950	1.27614	1.29894	1.30249	1.30332	1.33189	1.33983	1.34140	1.35175	1.35528	1.36073
30	c	-0.30286	-0.30657	-0.30642	-0.30609	-0.30581	-0.31043	-0.31030	-0.30997	-0.30969	-0.31018	-0.30985	-0.30957	-0.30952	-0.30924	-0.30896
	tr1	1.55087	1.63638	1.64065	1.64006	1.63898	1.77439	1.78929	1.78984	1.78894	1.81776	1.82205	1.82183	1.83153	1.83299	1.83691
	tr2	-0.26564	-0.22946	-0.22396	-0.22191	-0.22089	-0.20725	-0.19921	-0.19685	-0.19573	-0.19443	-0.19139	-0.19019	-0.18955	-0.18806	-0.18713
	tot	0.98237	1.10035	1.11027	1.11205	1.11229	1.25671	1.27978	1.28301	1.28352	1.31315	1.32081	1.32207	1.33246	1.33569	1.34083
35	c	-0.29603	-0.30113	-0.30096	-0.30052	-0.30014	-0.30648	-0.30633	-0.30589	-0.30551	-0.30619	-0.30575	-0.30537	-0.30531	-0.30494	-0.30456
	tr1	1.48188	1.57368	1.57768	1.57649	1.57493	1.71892	1.73366	1.73359	1.73216	1.76199	1.76567	1.76492	1.77449	1.77541	1.77876
	tr2	-0.22514	-0.18723	-0.18146	-0.17931	-0.17823	-0.16210	-0.15359	-0.15112	-0.14994	-0.14822	-0.14501	-0.14375	-0.14296	-0.14139	-0.14036
	tot	0.96071	1.08532	1.09526	1.09667	1.09656	1.25033	1.27373	1.27658	1.27670	1.30758	1.31490	1.31579	1.32622	1.32908	1.33384
40	c	-0.29195	-0.29873	-0.29852	-0.29796	-0.29747	-0.30590	-0.30573	-0.30516	-0.30466	-0.30556	-0.30500	-0.30451	-0.30443	-0.30394	-0.30345
	tr1	1.43210	1.53146	1.53516	1.53330	1.53176	1.68567	1.70027	1.69950	1.69744	1.72853	1.73149	1.73014	1.73958	1.73987	1.74255
	tr2	-0.19255	-0.15264	-0.14657	-0.14432	-0.14318	-0.12434	-0.11533	-0.11273	-0.11151	-0.10934	-0.10597	-0.10466	-0.10371	-0.10208	-0.10096
	tot	0.94760	1.08009	1.09060	1.09102	1.09051	1.25543	1.27922	1.28160	1.28127	1.31363	1.32053	1.32097	1.33144	1.33385	1.33813
45	c	-0.28962	-0.29837	-0.29813	-0.29741	-0.29680	-0.30771	-0.30752	-0.30680	-0.30617	-0.30734	-0.30662	-0.30599	-0.30590	-0.30528	-0.30465
	tr1	1.39815	1.50651	1.50991	1.50726	1.50446	1.67173	1.68623	1.68463	1.68185	1.71446	1.71660	1.71453	1.72983	1.72338	1.72528
	tr2	-0.16544	-0.12323	-0.11683	-0.11447	-0.11329	-0.09142	-0.08185	-0.07915	-0.07789	-0.07522	-0.07169	-0.07034	-0.06923	-0.06755	-0.06636
	tot	0.94309	1.08491	1.09494	1.09538	1.09438	1.27260	1.29685	1.29868	1.29779	1.33189	1.33829	1.33820	1.34868	1.35055	1.35427
50	c	-0.28966	-0.30076	-0.30049	-0.29960	-0.29882	-0.31274	-0.31253	-0.31162	-0.31083	-0.31233	-0.31143	-0.31063	-0.31053	-0.30974	-0.30895
	tr1	1.37825	1.49734	1.50041	1.49685	1.49328	1.67601	1.69042	1.68786	1.68422	1.71867	1.71985	1.71694	1.72607	1.72476	1.72574
	tr2	-0.14225	-0.09735	-0.09058	-0.08811	-0.08689	-0.06159	-0.05143	-0.04862	-0.04734	-0.04412	-0.04043	-0.03906	-0.03780	-0.03607	-0.03483
	tot	0.94635	1.09923	1.10934	1.10915	1.10757	1.30167	1.32646	1.32762	1.32606	1.36223	1.36799	1.36725	1.37774	1.37895	1.38197
55	c	-0.29187	-0.30578	-0.30546	-0.30435	-0.30339	-0.32095	-0.32071	-0.31957	-0.31858	-0.32048	-0.31936	-0.31836	-0.31823	-0.31725	-0.31626
	tr1	1.37139	1.50332	1.50602	1.50138	1.49690	1.69837	1.71273	1.70902	1.70435	1.74104	1.74107	1.73716	1.74609	1.74376	1.74364
	tr2	-0.12177	-0.07373	-0.06655	-0.06397	-0.06272	-0.03346	-0.02265	-0.01974	-0.01845	-0.01461	-0.01078	-0.00940	-0.00798	-0.00623	-0.00495
	tot	0.95775	1.12381	1.13401	1.13306	1.13080	1.34396	1.36937	1.36970	1.36732	1.40595	1.41094	1.41039	1.41988	1.42028	1.42243
60	c	-0.29655	-0.31383	-0.31346	-0.31209	-0.31091	-0.33290	-0.33262	-0.33121	-0.32997	-0.33237	-0.33097	-0.32973	-0.32957	-0.32834	-0.32711
	tr1	1.37742	1.52478	1.52707	1.52116	1.51560	1.73991	1.75421	1.74912	1.74320	1.78262	1.78127	1.77613	1.78485	1.78126	1.77983
	tr2	-0.10311	-0.05136	-0.04371	-0.04103	-0.03976	-0.00586	0.00568	0.00866	0.00994	0.01451	0.01846	0.01982	0.02140	0.02316	0.02445
	tot	0.97776	1.15959	1.16991	1.16804	1.16493	1.40115	1.42726	1.42657	1.42317	1.46476	1.46877	1.46623	1.47668	1.47608	1.47717
65	c	-0.30346	-0.32477	-0.32433	-0.32218	-0.32118	-0.34859	-0.34827	-0.34650	-0.34496	-0.34797	-0.34622	-0.34468	-0.34448	-0.34325	-0.34142
	tr1	1.39653	1.56256	1.56438	1.55692	1.55005	1.80235	1.81660	1.80981	1.80238	1.84514	1.84208	1.83546	1.84389	1.83879	1.83575
	tr2	-0.08548	-0.02930	-0.02110	-0.01834	-0.01707	0.02239	0.03473	0.03778	0.03900	0.04443	0.04849	0.04979	0.05155	0.05327	0.05453
	tot	1.00759	1.20849	1.21894	1.21594	1.21181	1.47615	1.50307	1.50108	1.49641	1.54161	1.54436	1.54057	1.55096	1.54911	1.54886
70	c	-0.31232	-0.33841	-0.33787	-0.33579	-0.33399	-0.36799	-0.36759	-0.36540	-0.36347	-0.36723	-0.36505	-0.36313	-0.36288	-0.36097	-0.35908
	tr1	1.42920	1.61795	1.61919	1.60986	1.60140	1.88822	1.90239	1.89347	1.88416	1.93107	1.92588	1.91740	1.92549	1.91850	1.91349
	tr2	-0.06814	-0.00659	0.00221	0.00504	0.00629	0.05251	0.06578	0.06683	0.06696	0.07644	0.08057	0.08176	0.08370	0.08534	0.08652
	tot	1.04875	1.27294	1.28353	1.27911	1.27370	1.57274	1.60058	1.59691	1.59065	1.64028	1.64140	1.63604	1.64632	1.64287	1.64094
75	c	-0.32549	-0.35759	-0.35691	-0.35433	-0.35211	-0.39453	-0.39402	-0.39126	-0.38884	-0.39356	-0.39082	-0.38841	-0.38809	-0.38571	-0.38333
	tr1	1.47873	1.69560	1.69615	1.68447	1.67403	2.00416	2.01820	2.00658	1.99487	2.04699	2.03920	2.02826	2.03592	2.02654	2.01905
	tr2	-0.05043	0.01769	0.02718	0.03006	0.03124	0.08588	0.10018	0.10320	0.10416	0.11193	0.11607	0.11710	0.11923	0.12071	0.12176
	tot	1.10281	1.35569	1.36642	1.36020	1.35316	1.69551	1.72436	1.71852	1.71020	1.76536	1.76435	1.75695	1.76706	1.76155	1.75747
80	c	-0.34201	-0.38148	-0.38061	-0.37740	-0.37464	-0.42763	-0.42697	-0.42346	-0.42041	-0.42636	-0.42288	-0.41984	-0.41944	-0.41643	-0.41344
	tr1	1.54661	1.79852	1.79817	1.78353											



TABLE II. Matrix elements of the operator  $h_{\text{h.o.}}^{\text{NMS}}$  for the  $np_{1/2}$  states calculated with the Dirac-Coulomb wave functions for the extended nuclei. The notations are the same as in Table I.

$Z$	Term	(2,2)	(2,3)	(2,4)	(2,5)	(3,3)	(3,4)	(3,5)	(4,4)	(4,5)	(5,5)
5	c	-0.000 21	-0.000 22	-0.000 23	-0.000 23	-0.000 24	-0.000 25	-0.000 25	-0.000 26	-0.000 26	-0.000 26
	tr1	-0.047 48	-0.047 34	-0.049 21	-0.050 21	-0.041 34	-0.041 70	-0.042 96	-0.038 43	-0.038 63	-0.036 79
	tr2	-0.038 02	-0.033 95	-0.033 02	-0.032 64	-0.035 70	-0.034 42	-0.034 00	-0.034 89	-0.034 32	-0.034 51
	tot	-0.085 70	-0.081 51	-0.082 46	-0.083 08	-0.077 29	-0.076 37	-0.077 20	-0.073 57	-0.073 20	-0.071 56
10	c	-0.000 76	-0.000 83	-0.000 85	-0.000 86	-0.000 90	-0.000 92	-0.000 93	-0.000 95	-0.000 96	-0.000 97
	tr1	-0.048 58	-0.048 67	-0.050 59	-0.051 62	-0.042 94	-0.043 37	-0.044 65	-0.040 19	-0.040 42	-0.038 63
	tr2	-0.023 13	-0.018 17	-0.017 02	-0.016 54	-0.018 55	-0.016 93	-0.016 39	-0.016 95	-0.016 22	-0.016 20
	tot	-0.072 47	-0.067 67	-0.068 47	-0.069 02	-0.062 39	-0.061 22	-0.061 97	-0.058 08	-0.057 59	-0.055 80
15	c	-0.001 61	-0.001 75	-0.001 80	-0.001 82	-0.001 91	-0.001 96	-0.001 98	-0.002 01	-0.002 03	-0.002 05
	tr1	-0.048 87	-0.049 08	-0.051 02	-0.052 04	-0.043 48	-0.043 94	-0.045 22	-0.040 81	-0.041 05	-0.039 28
	tr2	-0.008 21	-0.002 37	-0.001 00	-0.000 43	-0.001 38	0.000 58	0.001 24	0.001 01	0.001 90	0.002 11
	tot	-0.058 69	-0.053 20	-0.053 82	-0.054 29	-0.046 76	-0.045 32	-0.045 96	-0.041 81	-0.041 18	-0.039 22
20	c	-0.002 74	-0.002 98	-0.003 06	-0.003 09	-0.003 24	-0.003 32	-0.003 36	-0.003 41	-0.003 45	-0.003 49
	tr1	-0.048 49	-0.048 73	-0.050 64	-0.051 65	-0.043 15	-0.043 60	-0.044 86	-0.040 48	-0.040 71	-0.038 95
	tr2	0.006 94	0.013 66	0.015 24	0.015 89	0.016 04	0.018 32	0.019 10	0.019 20	0.020 24	0.020 65
	tot	-0.044 30	-0.038 04	-0.038 46	-0.038 85	-0.030 36	-0.028 60	-0.029 12	-0.024 69	-0.023 92	-0.021 78
25	c	-0.004 16	-0.004 51	-0.004 63	-0.004 68	-0.004 90	-0.005 02	-0.005 08	-0.005 15	-0.005 21	-0.005 26
	tr1	-0.047 52	-0.047 68	-0.049 54	-0.050 52	-0.042 03	-0.042 43	-0.043 65	-0.039 28	-0.039 48	-0.037 71
	tr2	0.022 47	0.030 10	0.031 87	0.032 60	0.033 88	0.036 49	0.037 37	0.037 81	0.038 99	0.039 59
	tot	-0.029 21	-0.022 09	-0.022 30	-0.022 60	-0.013 05	-0.010 96	-0.011 35	-0.006 62	-0.005 69	-0.003 38
30	c	-0.005 87	-0.006 36	-0.006 52	-0.006 59	-0.006 90	-0.007 07	-0.007 15	-0.007 25	-0.007 33	-0.007 40
	tr1	-0.045 96	-0.045 95	-0.047 72	-0.048 66	-0.040 12	-0.040 44	-0.041 60	-0.037 23	-0.037 39	-0.035 60
	tr2	0.038 57	0.047 13	0.049 09	0.049 89	0.052 36	0.055 30	0.056 27	0.057 05	0.058 38	0.059 16
	tot	-0.013 26	-0.005 18	-0.005 15	-0.005 36	0.005 34	0.007 78	0.007 52	0.012 57	0.013 67	0.016 16
35	c	-0.007 91	-0.008 57	-0.008 78	-0.008 87	-0.009 29	-0.009 52	-0.009 61	-0.009 75	-0.009 85	-0.009 94
	tr1	-0.043 78	-0.043 50	-0.045 15	-0.046 03	-0.037 39	-0.037 59	-0.038 67	-0.034 30	-0.034 39	-0.032 57
	tr2	0.055 45	0.064 97	0.067 11	0.067 96	0.071 72	0.074 97	0.076 03	0.077 17	0.078 62	0.079 57
	tot	0.003 77	0.012 90	0.013 18	0.013 06	0.025 04	0.027 86	0.027 74	0.033 12	0.034 39	0.037 06
40	c	-0.010 35	-0.011 21	-0.011 47	-0.011 58	-0.012 14	-0.012 42	-0.012 54	-0.012 71	-0.012 83	-0.012 96
	tr1	-0.040 88	-0.040 23	-0.041 72	-0.042 52	-0.033 73	-0.033 78	-0.034 76	-0.030 36	-0.030 37	-0.028 51
	tr2	0.073 35	0.083 87	0.086 17	0.087 05	0.092 21	0.095 78	0.096 90	0.098 41	0.099 98	0.101 09
	tot	0.022 11	0.032 43	0.032 98	0.032 95	0.046 34	0.049 57	0.049 60	0.055 33	0.056 77	0.059 63
45	c	-0.013 24	-0.014 33	-0.014 65	-0.014 78	-0.015 51	-0.015 86	-0.016 00	-0.016 22	-0.016 36	-0.016 51
	tr1	-0.037 14	-0.036 00	-0.037 28	-0.037 99	-0.028 97	-0.028 83	-0.029 70	-0.025 26	-0.025 17	-0.023 26
	tr2	0.092 53	0.104 12	0.106 55	0.107 45	0.114 16	0.118 03	0.119 20	0.121 10	0.122 76	0.124 02
	tot	0.042 14	0.053 79	0.054 62	0.054 68	0.069 67	0.073 33	0.073 50	0.079 62	0.081 23	0.084 26
50	c	-0.016 71	-0.018 07	-0.018 45	-0.018 60	-0.019 54	-0.019 96	-0.020 12	-0.020 39	-0.020 56	-0.020 73
	tr1	-0.032 34	-0.030 56	-0.031 59	-0.032 19	-0.022 86	-0.022 49	-0.023 22	-0.018 72	-0.018 53	-0.016 55
	tr2	0.113 34	0.126 07	0.128 61	0.129 49	0.137 94	0.142 10	0.143 29	0.145 61	0.147 35	0.148 73
	tot	0.064 29	0.077 45	0.078 57	0.078 70	0.095 54	0.099 65	0.099 95	0.106 49	0.108 26	0.111 45
55	c	-0.020 89	-0.022 56	-0.023 02	-0.023 19	-0.024 37	-0.024 87	-0.025 05	-0.025 38	-0.025 57	-0.025 76
	tr1	-0.026 18	-0.023 57	-0.024 30	-0.024 76	-0.015 03	-0.014 38	-0.014 94	-0.010 38	-0.010 05	-0.008 01
	tr2	0.136 21	0.150 16	0.152 78	0.153 61	0.164 02	0.168 46	0.169 64	0.172 40	0.174 18	0.175 66
	tot	0.089 14	0.104 03	0.105 47	0.105 66	0.124 62	0.129 21	0.129 64	0.136 64	0.138 56	0.141 89
60	c	-0.025 97	-0.028 01	-0.028 55	-0.028 74	-0.030 23	-0.030 82	-0.031 02	-0.031 42	-0.031 63	-0.031 84
	tr1	-0.018 21	-0.014 56	-0.014 91	-0.015 23	-0.004 95	-0.003 96	-0.004 34	0.000 32	0.000 78	0.002 90
	tr2	0.161 66	0.176 94	0.179 60	0.180 33	0.193 01	0.197 71	0.198 82	0.202 07	0.203 86	0.205 40
	tot	0.117 48	0.134 37	0.136 14	0.136 36	0.157 82	0.162 93	0.163 46	0.170 97	0.173 01	0.176 46
65	c	-0.032 20	-0.034 68	-0.035 31	-0.035 50	-0.037 39	-0.038 07	-0.038 28	-0.038 76	-0.038 98	-0.039 20
	tr1	-0.007 82	-0.002 83	-0.002 73	-0.002 87	0.008 12	0.009 52	0.009 35	0.014 12	0.014 74	0.016 93
	tr2	0.190 40	0.207 15	0.209 79	0.210 35	0.225 67	0.230 60	0.231 59	0.235 37	0.237 11	0.238 67
	tot	0.150 39	0.169 64	0.171 75	0.171 97	0.196 40	0.202 05	0.202 66	0.210 73	0.212 87	0.216 39
70	c	-0.039 86	-0.042 88	-0.043 59	-0.043 79	-0.046 17	-0.046 94	-0.047 16	-0.047 73	-0.047 95	-0.048 17
	tr1	0.005 89	0.012 57	0.013 22	0.013 27	0.025 24	0.027 10	0.027 17	0.032 09	0.032 86	0.035 12
	tr2	0.223 32	0.241 72	0.244 25	0.244 57	0.263 02	0.268 13	0.268 92	0.273 29	0.274 92	0.276 42
	tot	0.189 35	0.211 41	0.213 88	0.214 05	0.242 09	0.248 29	0.248 93	0.257 64	0.259 83	0.263 37
75	c	-0.049 60	-0.053 28	-0.054 08	-0.054 26	-0.057 29	-0.058 16	-0.058 36	-0.059 05	-0.059 25	-0.059 46
	tr1	0.024 29	0.033 18	0.034 49	0.034 74	0.048 06	0.050 47	0.050 78	0.055 90	0.056 83	0.059 12
	tr2	0.261 68	0.281 94	0.284 26	0.284 22	0.306 42	0.311 65	0.312 14	0.317 16	0.318 58	0.319 95
	tot	0.236 37	0.261 84	0.264 67	0.264 70	0.297 20	0.303 96	0.304 56	0.314 01	0.316 16	0.319 62
80	c	-0.062 00	-0.066 50	-0.067 38	-0.067 51	-0.071 39	-0.072 35	-0.072 50	-0.073 33	-0.073 49	-0.073 65
	tr1	0.049 34	0.061 11	0.063 19	0.063 66	0.078 85	0.081 90	0.082 45	0.087 82	0.088 88	0.091 18
	tr2	0.307 16	0.329 55	0.331 51	0.330 95	0.357 75	0.362 99	0.363 02	0.368 79	0.369 87	0.370 98
	tot	0.294 49	0.324 16	0.327 32	0.327 10	0.365 21	0.372 54	0.372 97	0.383 28	0.385 26	0.388 51
85	c	-0.078 11	-0.083 62	-0.084 56	-0.084 61	-0.089 62	-0.090 65	-0.090 71	-0.091 70	-0.091 76	-0.091 83
	tr1	0.084 05	0.099 64	0.102 65	0.103 31	0.121 15	0.124 92	0.125 68	0.131 39	0.132 52	0.134 74
	tr2	0.362 14	0.387 02	0.388 39	0.387 12	0.419 60	0.424 71	0.424 08	0.430 70	0.431 24	0.431 93
	tot	0.368 07	0.403 04	0.406 48	0.405 82	0.451 13	0.458 97	0.459 05	0.470 40	0.472 00	0.474 83
90	c	-0.098 98	-0.105 73	-0.106 68	-0.106 56	-0.113 08	-0.114 12	-0.114 01	-0.115 19	-0.115 08	-0.114 98
	tr1	0.132 64	0.153 30	0.157 37	0.158 15	0.179 78	0.184 33	0.185 22	0.191 38	0.192 44	0.194 41
	tr2	0.429 94	0.457 76	0.458 22	0.455 91	0.495 59	0.500 32	0.498 72	0.506 33	0.506 06	0.506 05
	tot	0.463 60	0.505 33	0.508 91	0.507 50	0.562 30	0.570 53	0.569 92	0.582 51	0.583 41	0.585 49
95	c	-0.127 26	-0.135 59	-0.136 45	-0.136 05	-0.144 66	-0.145 63	-0.145 22	-0.146 62	-0.146 22	-0.145 81
	tr1	0.202 82	0.230 40	0.235 64	0.236 35	0.263 61	0.268 94	0.269 73	0.276 49	0.277 22	0.278 67
	tr2	0.515 74	0.547 05	0.546 10	0.542 32	0.591 28	0.595 25	0.592 23	0.600 99	0.599 48	0.598 41
	tot	0.591 30	0.641 86	0.645 29	0.642 63	0.710 23	0.718 56	0.716 74	0.730 85	0.730 49	0.731 26
100	c	-0.166 93	-0.177 34	-0.177 94	-0.177 03	-0.188 67	-0.189 38	-0.188 44	-0.190 12	-0.189 19	-0.188 27
	tr1	0.307 52	0.344 73	0.351 15	0.351 41	0.387 25	0.393 20	0.393 45	0.401 03	0.400 91	0.401 29
	tr2	0.627 54	0.663 10	0.659 98	0.654 01	0.715 27	0.717 85	0.712 70	0.722 81	0.719 43	0.716 67
	tot	0.768 12	0.830 49	0.833 19	0.828 39	0.913 85	0.921 67	0.917 70	0.933 72	0.931 15	0.929 69

TABLE III. Matrix elements of the operator  $h_{\text{h.o.}}^{\text{NMS}}$  for the  $np_{3/2}$  states calculated with the Dirac-Coulomb wave functions for the extended nuclei. The notations are the same as in Table I.

Z	Term	(2,2)	(2,3)	(2,4)	(2,5)	(3,3)	(3,4)	(3,5)	(4,4)	(4,5)	(5,5)
5	c	-0.000 04	-0.000 04	-0.000 05	-0.000 05	-0.000 05	-0.000 05	-0.000 05	-0.000 05	-0.000 05	-0.000 05
	tr1	-0.039 16	-0.038 65	-0.040 38	-0.041 32	-0.032 21	-0.032 43	-0.033 62	-0.029 01	-0.029 15	-0.027 24
	tr2	-0.047 51	-0.043 89	-0.043 11	-0.042 79	-0.046 28	-0.045 17	-0.044 83	-0.045 85	-0.045 36	-0.045 65
	tot	-0.086 71	-0.082 59	-0.083 54	-0.084 16	-0.078 54	-0.077 65	-0.078 50	-0.074 91	-0.074 56	-0.072 94
10	c	-0.000 13	-0.000 15	-0.000 15	-0.000 15	-0.000 16	-0.000 16	-0.000 16	-0.000 17	-0.000 17	-0.000 17
	tr1	-0.033 00	-0.032 50	-0.034 21	-0.035 13	-0.026 01	-0.026 22	-0.027 40	-0.022 79	-0.022 92	-0.021 01
	tr2	-0.042 60	-0.038 59	-0.037 74	-0.037 40	-0.040 29	-0.039 04	-0.038 65	-0.039 47	-0.038 92	-0.039 09
	tot	-0.075 73	-0.071 23	-0.072 10	-0.072 69	-0.066 46	-0.065 42	-0.066 22	-0.062 43	-0.062 01	-0.060 27
15	c	-0.000 25	-0.000 28	-0.000 28	-0.000 29	-0.000 30	-0.000 31	-0.000 31	-0.000 31	-0.000 32	-0.000 32
	tr1	-0.026 78	-0.026 30	-0.027 99	-0.028 90	-0.019 73	-0.019 93	-0.021 11	-0.016 48	-0.016 60	-0.014 68
	tr2	-0.038 14	-0.033 77	-0.032 88	-0.032 51	-0.034 83	-0.033 44	-0.033 03	-0.033 66	-0.033 04	-0.033 11
	tot	-0.065 17	-0.060 34	-0.061 15	-0.061 70	-0.054 85	-0.053 68	-0.054 44	-0.050 45	-0.049 96	-0.048 11
20	c	-0.000 39	-0.000 42	-0.000 43	-0.000 44	-0.000 46	-0.000 47	-0.000 47	-0.000 48	-0.000 48	-0.000 49
	tr1	-0.020 51	-0.020 04	-0.021 73	-0.022 64	-0.013 37	-0.013 57	-0.014 74	-0.010 08	-0.010 20	-0.008 26
	tr2	-0.034 03	-0.029 34	-0.028 41	-0.028 03	-0.029 79	-0.028 28	-0.027 84	-0.028 28	-0.027 60	-0.027 58
	tot	-0.054 93	-0.049 80	-0.050 57	-0.051 10	-0.043 61	-0.042 31	-0.043 05	-0.038 84	-0.038 29	-0.036 33
25	c	-0.000 53	-0.000 58	-0.000 59	-0.000 59	-0.000 62	-0.000 64	-0.000 64	-0.000 65	-0.000 66	-0.000 67
	tr1	-0.014 18	-0.013 74	-0.015 42	-0.016 33	-0.006 93	-0.007 12	-0.008 29	-0.003 59	-0.003 70	-0.001 74
	tr2	-0.030 25	-0.025 26	-0.024 29	-0.023 90	-0.025 11	-0.023 48	-0.023 02	-0.023 28	-0.022 55	-0.022 43
	tot	-0.044 97	-0.039 57	-0.040 30	-0.040 83	-0.032 66	-0.031 24	-0.031 95	-0.027 52	-0.026 91	-0.024 84
30	c	-0.000 68	-0.000 73	-0.000 75	-0.000 76	-0.000 79	-0.000 81	-0.000 82	-0.000 83	-0.000 84	-0.000 84
	tr1	-0.007 80	-0.007 37	-0.009 06	-0.009 98	-0.000 39	-0.000 57	-0.001 75	0.003 02	0.002 91	0.004 90
	tr2	-0.026 77	-0.021 49	-0.020 49	-0.020 10	-0.020 77	-0.019 03	-0.018 54	-0.018 63	-0.017 84	-0.017 63
	tot	-0.035 25	-0.029 59	-0.030 31	-0.030 83	-0.021 95	-0.020 41	-0.021 11	-0.016 44	-0.015 77	-0.013 58
35	c	-0.000 83	-0.000 89	-0.000 91	-0.000 92	-0.000 96	-0.000 98	-0.000 99	-0.001 01	-0.001 02	-0.001 03
	tr1	-0.001 34	-0.000 92	-0.002 63	-0.003 56	0.006 27	0.006 10	0.004 92	0.009 77	0.009 66	0.011 68
	tr2	-0.023 58	-0.018 02	-0.017 00	-0.016 60	-0.016 74	-0.014 89	-0.014 39	-0.014 30	-0.013 45	-0.013 16
	tot	-0.025 75	-0.019 84	-0.020 55	-0.021 08	-0.011 43	-0.009 77	-0.010 46	-0.005 54	-0.004 81	-0.002 50
40	c	-0.000 97	-0.001 05	-0.001 07	-0.001 08	-0.001 13	-0.001 16	-0.001 17	-0.001 18	-0.001 19	-0.001 20
	tr1	0.005 20	0.005 62	0.003 89	0.002 95	0.013 08	0.012 93	0.011 73	0.016 68	0.016 58	0.018 65
	tr2	-0.020 67	-0.014 85	-0.013 81	-0.013 41	-0.013 02	-0.011 06	-0.010 54	-0.010 27	-0.009 38	-0.008 99
	tot	-0.016 45	-0.010 28	-0.011 00	-0.011 54	-0.001 07	0.000 71	0.000 02	0.005 22	0.006 01	0.008 45
45	c	-0.001 12	-0.001 21	-0.001 23	-0.001 24	-0.001 30	-0.001 33	-0.001 34	-0.001 36	-0.001 37	-0.001 38
	tr1	0.011 84	0.012 28	0.010 52	0.009 56	0.020 07	0.019 94	0.018 72	0.023 80	0.023 71	0.025 82
	tr2	-0.018 06	-0.011 98	-0.010 92	-0.010 51	-0.009 60	-0.007 54	-0.007 00	-0.006 56	-0.005 61	-0.005 14
	tot	-0.007 34	-0.000 90	-0.001 64	-0.002 19	0.009 17	0.011 07	0.010 38	0.015 88	0.016 73	0.019 30
50	c	-0.001 27	-0.001 36	-0.001 39	-0.001 40	-0.001 47	-0.001 50	-0.001 51	-0.001 53	-0.001 55	-0.001 56
	tr1	0.018 61	0.019 10	0.017 29	0.016 31	0.027 27	0.027 17	0.025 93	0.031 16	0.031 08	0.033 26
	tr2	-0.015 74	-0.009 41	-0.008 34	-0.007 93	-0.006 48	-0.004 32	-0.003 77	-0.003 15	-0.002 16	-0.001 60
	tot	0.001 60	0.008 33	0.007 57	0.006 98	0.019 32	0.021 35	0.020 64	0.026 48	0.027 38	0.030 10
55	c	-0.001 41	-0.001 52	-0.001 55	-0.001 56	-0.001 63	-0.001 67	-0.001 68	-0.001 71	-0.001 72	-0.001 74
	tr1	0.025 52	0.026 08	0.024 24	0.023 22	0.034 73	0.034 66	0.033 40	0.038 81	0.038 75	0.041 00
	tr2	-0.013 74	-0.007 15	-0.006 06	-0.005 65	-0.003 69	-0.001 42	-0.000 86	-0.000 06	0.000 98	0.001 63
	tot	0.010 37	0.017 42	0.016 63	0.016 01	0.029 40	0.031 57	0.030 86	0.037 05	0.038 01	0.040 89
60	c	-0.001 56	-0.001 67	-0.001 71	-0.001 72	-0.001 80	-0.001 84	-0.001 86	-0.001 88	-0.001 90	-0.001 92
	tr1	0.032 61	0.033 28	0.031 39	0.030 34	0.042 48	0.042 47	0.041 18	0.046 81	0.046 77	0.049 09
	tr2	-0.012 07	-0.005 21	-0.004 12	-0.003 70	-0.001 22	0.001 15	0.001 72	0.002 70	0.003 79	0.004 52
	tot	0.018 99	0.026 40	0.025 57	0.024 91	0.039 46	0.041 78	0.041 04	0.047 63	0.048 66	0.051 70
65	c	-0.001 70	-0.001 83	-0.001 87	-0.001 88	-0.001 97	-0.002 02	-0.002 03	-0.002 06	-0.002 08	-0.002 10
	tr1	0.039 90	0.040 73	0.038 79	0.037 69	0.050 59	0.050 65	0.049 33	0.055 21	0.055 20	0.057 62
	tr2	-0.010 74	-0.003 62	-0.002 51	-0.002 10	0.000 89	0.003 36	0.003 95	0.005 11	0.006 24	0.007 06
	tot	0.027 46	0.035 28	0.034 41	0.033 71	0.049 51	0.052 00	0.051 25	0.058 26	0.059 36	0.062 58
70	c	-0.001 85	-0.001 99	-0.002 03	-0.002 04	-0.002 15	-0.002 19	-0.002 21	-0.002 24	-0.002 26	-0.002 28
	tr1	0.047 42	0.048 47	0.046 47	0.045 33	0.059 10	0.059 26	0.057 91	0.064 08	0.064 10	0.066 63
	tr2	-0.009 78	-0.002 40	-0.001 27	-0.000 86	0.002 62	0.005 20	0.005 80	0.007 14	0.008 32	0.009 22
	tot	0.035 80	0.044 09	0.043 17	0.042 43	0.059 58	0.062 27	0.061 50	0.068 97	0.070 16	0.073 57
75	c	-0.002 00	-0.002 15	-0.002 19	-0.002 21	-0.002 32	-0.002 37	-0.002 39	-0.002 43	-0.002 45	-0.002 47
	tr1	0.055 20	0.056 54	0.054 49	0.053 29	0.068 09	0.068 37	0.066 99	0.073 49	0.073 56	0.076 21
	tr2	-0.009 21	-0.001 56	-0.000 42	0.000 00	0.003 95	0.006 64	0.007 25	0.008 76	0.010 00	0.010 98
	tot	0.044 00	0.052 83	0.051 88	0.051 08	0.069 72	0.072 64	0.071 84	0.079 82	0.081 11	0.084 72
80	c	-0.002 15	-0.002 31	-0.002 36	-0.002 37	-0.002 51	-0.002 56	-0.002 58	-0.002 62	-0.002 64	-0.002 66
	tr1	0.063 29	0.065 00	0.062 90	0.061 64	0.077 62	0.078 05	0.076 64	0.083 52	0.083 65	0.086 45
	tr2	-0.009 05	-0.001 15	0.000 01	0.000 44	0.004 84	0.007 63	0.008 25	0.009 94	0.011 22	0.012 29
	tot	0.052 09	0.061 54	0.060 56	0.059 70	0.079 95	0.083 12	0.082 31	0.090 84	0.092 23	0.096 07
85	c	-0.002 30	-0.002 48	-0.002 53	-0.002 55	-0.002 70	-0.002 76	-0.002 78	-0.002 82	-0.002 84	-0.002 87
	tr1	0.071 71	0.073 90	0.071 75	0.070 43	0.087 76	0.088 39	0.086 95	0.094 27	0.094 48	0.097 44
	tr2	-0.009 36	-0.001 19	0.000 00	0.000 43	0.005 24	0.008 14	0.008 77	0.010 63	0.011 96	0.013 10
	tot	0.060 05	0.070 23	0.069 22	0.068 31	0.090 30	0.093 77	0.092 94	0.102 08	0.103 59	0.107 68
90	c	-0.002 46	-0.002 66	-0.002 71	-0.002 73	-0.002 90	-0.002 96	-0.002 99	-0.003 03	-0.003 06	-0.003 08
	tr1	0.080 50	0.083 29	0.081 11	0.079 72	0.098 59	0.099 47	0.098 01	0.105 82	0.106 12	0.109 28
	tr2	-0.010 14	-0.001 73	-0.000 51	-0.000 06	0.005 10	0.008 10	0.008 75	0.010 76	0.012 14	0.013 36
	tot	0.067 89	0.078 90	0.077 89	0.076 92	0.100 79	0.104 61	0.103 77	0.113 55	0.115 21	0.119 56
95	c	-0.002 63	-0.002 85	-0.002 91	-0.002 93	-0.003 11	-0.003 18	-0.003 21	-0.003 26	-0.003 28	-0.003 31
	tr1	0.089 69	0.093 24	0.091 04	0.089 58	0.110 20	0.111 39	0.109 92	0.118 28	0.118 71	0.122 08
	tr2	-0.011 46	-0.002 80	-0.001 55	-0.001 09	0.004 36	0.007 46	0.008 12	0.010 29	0.011 71	0.013 01
	tot	0.075 61	0.087 59	0.086 59	0.085 56	0.111 45	0.115 67	0.114 83	0.125 31	0.127 14	0.131 77
100	c	-0.002 81	-0.003 05	-0.003 11	-0.003 13	-0.003 34	-0.003 42	-0.003 44	-0.003 50	-0.003 53	-0.003 56
	tr1	0.099 35	0.103 82	0.101 63	0.100 10	0.122 68	0.124 27	0.122 80	0.131 78	0.132 36	0.135 97
	tr2	-0.013 34	-0.004 48	-0.003 18	-0.002 70	0.002 95	0.006 14	0.006 82	0.009 11	0.010 58	0.011 94
	tot	0.083 20	0.096 29	0.095 34	0.094 26	0.122 30	0.127 00	0.126 17	0.137 39	0.139 41	0.144 35

TABLE IV. Matrix elements of the operator  $h_{\text{h.o.}}^{\text{NMS}}$  for the  $nd_{3/2}$  states calculated with the Dirac-Coulomb wave functions for the extended nuclei. The notations are the same as in Table I.

Z	Term	(3,3)	(3,4)	(3,5)	(4,4)	(4,5)	(5,5)
5	c	0.00000	0.00000	0.00000	0.00000	0.00000	0.00000
	tr1	-0.00932	-0.00918	-0.00969	-0.00814	-0.00840	-0.00746
	tr2	-0.00938	-0.00796	-0.00756	-0.00908	-0.00853	-0.00894
	tot	-0.01870	-0.01713	-0.01726	-0.01722	-0.01693	-0.01639
10	c	0.00000	0.00000	0.00000	0.00000	0.00000	0.00000
	tr1	-0.00896	-0.00889	-0.00944	-0.00789	-0.00817	-0.00725
	tr2	-0.00814	-0.00664	-0.00624	-0.00753	-0.00694	-0.00724
	tot	-0.01710	-0.01553	-0.01568	-0.01541	-0.01511	-0.01450
15	c	0.00000	0.00000	0.00000	0.00000	0.00000	0.00000
	tr1	-0.00862	-0.00864	-0.00921	-0.00766	-0.00798	-0.00707
	tr2	-0.00688	-0.00531	-0.00491	-0.00596	-0.00533	-0.00554
	tot	-0.01550	-0.01395	-0.01412	-0.01362	-0.01331	-0.01261
20	c	0.00000	0.00000	0.00000	0.00000	0.00000	-0.00001
	tr1	-0.00830	-0.00840	-0.00900	-0.00745	-0.00780	-0.00691
	tr2	-0.00561	-0.00397	-0.00357	-0.00438	-0.00371	-0.00382
	tot	-0.01392	-0.01238	-0.01258	-0.01184	-0.01151	-0.01073
25	c	-0.00001	-0.00001	-0.00001	-0.00001	-0.00001	-0.00001
	tr1	-0.00799	-0.00818	-0.00881	-0.00724	-0.00763	-0.00676
	tr2	-0.00433	-0.00262	-0.00222	-0.00279	-0.00208	-0.00208
	tot	-0.01233	-0.01081	-0.01104	-0.01005	-0.00972	-0.00885
30	c	-0.00001	-0.00001	-0.00001	-0.00001	-0.00002	-0.00002
	tr1	-0.00769	-0.00797	-0.00864	-0.00705	-0.00747	-0.00661
	tr2	-0.00304	-0.00125	-0.00085	-0.00118	-0.00042	-0.00032
	tot	-0.01074	-0.00923	-0.00951	-0.00825	-0.00791	-0.00695
35	c	-0.00002	-0.00002	-0.00002	-0.00002	-0.00002	-0.00003
	tr1	-0.00739	-0.00776	-0.00848	-0.00685	-0.00732	-0.00646
	tr2	-0.00173	0.00013	0.00053	0.00045	0.00125	0.00145
	tot	-0.00913	-0.00765	-0.00797	-0.00643	-0.00609	-0.00503
40	c	-0.00002	-0.00003	-0.00003	-0.00003	-0.00004	-0.00004
	tr1	-0.00708	-0.00756	-0.00831	-0.00665	-0.00715	-0.00630
	tr2	-0.00041	0.00153	0.00193	0.00210	0.00295	0.00326
	tot	-0.00751	-0.00605	-0.00641	-0.00459	-0.00424	-0.00308
45	c	-0.00003	-0.00004	-0.00004	-0.00005	-0.00005	-0.00005
	tr1	-0.00677	-0.00734	-0.00815	-0.00643	-0.00698	-0.00612
	tr2	0.00094	0.00296	0.00335	0.00378	0.00468	0.00509
	tot	-0.00587	-0.00442	-0.00483	-0.00270	-0.00235	-0.00108
50	c	-0.00005	-0.00005	-0.00006	-0.00006	-0.00007	-0.00007
	tr1	-0.00644	-0.00711	-0.00797	-0.00619	-0.00678	-0.00591
	tr2	0.00230	0.00440	0.00480	0.00549	0.00643	0.00696
	tot	-0.00418	-0.00276	-0.00323	-0.00077	-0.00041	0.00098
55	c	-0.00006	-0.00007	-0.00008	-0.00008	-0.00009	-0.00009
	tr1	-0.00609	-0.00686	-0.00777	-0.00592	-0.00654	-0.00566
	tr2	0.00369	0.00588	0.00627	0.00723	0.00823	0.00886
	tot	-0.00246	-0.00105	-0.00158	0.00124	0.00160	0.00311
60	c	-0.00008	-0.00009	-0.00010	-0.00011	-0.00011	-0.00012
	tr1	-0.00570	-0.00657	-0.00755	-0.00559	-0.00626	-0.00536
	tr2	0.00511	0.00738	0.00777	0.00902	0.01006	0.01081
	tot	-0.00068	0.00072	0.00013	0.00332	0.00369	0.00533
65	c	-0.00010	-0.00012	-0.00012	-0.00013	-0.00014	-0.00015
	tr1	-0.00528	-0.00624	-0.00728	-0.00521	-0.00592	-0.00499
	tr2	0.00655	0.00892	0.00931	0.01084	0.01194	0.01281
	tot	0.00117	0.00256	0.00190	0.00550	0.00588	0.00767
70	c	-0.00012	-0.00014	-0.00015	-0.00017	-0.00018	-0.00019
	tr1	-0.00480	-0.00585	-0.00696	-0.00475	-0.00549	-0.00452
	tr2	0.00802	0.01049	0.01087	0.01272	0.01386	0.01486
	tot	0.00310	0.00450	0.00376	0.00779	0.00820	0.01015
75	c	-0.00015	-0.00018	-0.00019	-0.00020	-0.00022	-0.00023
	tr1	-0.00426	-0.00538	-0.00657	-0.00420	-0.00496	-0.00394
	tr2	0.00953	0.01210	0.01248	0.01463	0.01584	0.01696
	tot	0.00512	0.00654	0.00573	0.01023	0.01066	0.01279
80	c	-0.00018	-0.00021	-0.00023	-0.00025	-0.00026	-0.00028
	tr1	-0.00363	-0.00482	-0.00608	-0.00352	-0.00430	-0.00322
	tr2	0.01107	0.01374	0.01412	0.01660	0.01787	0.01912
	tot	0.00726	0.00871	0.00781	0.01284	0.01330	0.01562
85	c	-0.00022	-0.00026	-0.00027	-0.00030	-0.00032	-0.00033
	tr1	-0.00289	-0.00413	-0.00548	-0.00268	-0.00347	-0.00231
	tr2	0.01264	0.01542	0.01580	0.01862	0.01994	0.02133
	tot	0.00952	0.01103	0.01005	0.01564	0.01616	0.01869
90	c	-0.00026	-0.00031	-0.00032	-0.00036	-0.00038	-0.00040
	tr1	-0.00202	-0.00329	-0.00472	-0.00165	-0.00244	-0.00117
	tr2	0.01423	0.01714	0.01751	0.02068	0.02207	0.02359
	tot	0.01195	0.01354	0.01247	0.01868	0.01926	0.02203
95	c	-0.00031	-0.00036	-0.00038	-0.00042	-0.00045	-0.00047
	tr1	-0.00100	-0.00226	-0.00377	-0.00038	-0.00114	0.00025
	tr2	0.01585	0.01889	0.01925	0.02279	0.02424	0.02590
	tot	0.01455	0.01626	0.01510	0.02199	0.02265	0.02568
100	c	-0.00037	-0.00043	-0.00045	-0.00050	-0.00052	-0.00055
	tr1	0.00023	-0.00098	-0.00257	0.00119	0.00048	0.00202
	tr2	0.01749	0.02065	0.02101	0.02492	0.02644	0.02825
	tot	0.01735	0.01924	0.01798	0.02562	0.02639	0.02972

TABLE V. Matrix elements of the operator  $h_{\text{h.o.}}^{\text{NMS}}$  for the  $nd_{5/2}$  states calculated with the Dirac-Coulomb wave functions for the extended nuclei. The notations are the same as in Table I.

Z	Term	(3,3)	(3,4)	(3,5)	(4,4)	(4,5)	(5,5)
5	c	0.00000	0.00000	0.00000	0.00000	0.00000	0.00000
	tr1	-0.00863	-0.00846	-0.00896	-0.00737	-0.00761	-0.00665
	tr2	-0.01006	-0.00865	-0.00826	-0.00984	-0.00931	-0.00974
	tot	-0.01869	-0.01711	-0.01722	-0.01721	-0.01692	-0.01639
10	c	0.00000	0.00000	0.00000	0.00000	0.00000	0.00000
	tr1	-0.00756	-0.00744	-0.00794	-0.00632	-0.00656	-0.00560
	tr2	-0.00951	-0.00804	-0.00766	-0.00907	-0.00851	-0.00887
	tot	-0.01707	-0.01548	-0.01560	-0.01539	-0.01508	-0.01448
15	c	0.00000	0.00000	0.00000	0.00000	0.00000	0.00000
	tr1	-0.00650	-0.00642	-0.00693	-0.00527	-0.00552	-0.00456
	tr2	-0.00896	-0.00743	-0.00705	-0.00831	-0.00772	-0.00801
	tot	-0.01545	-0.01385	-0.01398	-0.01358	-0.01325	-0.01257
20	c	0.00000	0.00000	0.00000	0.00000	0.00000	0.00000
	tr1	-0.00543	-0.00540	-0.00592	-0.00421	-0.00448	-0.00351
	tr2	-0.00841	-0.00683	-0.00646	-0.00756	-0.00694	-0.00716
	tot	-0.01384	-0.01223	-0.01238	-0.01177	-0.01142	-0.01067
25	c	0.00000	0.00000	0.00000	-0.00001	-0.00001	-0.00001
	tr1	-0.00436	-0.00438	-0.00491	-0.00316	-0.00344	-0.00246
	tr2	-0.00787	-0.00624	-0.00588	-0.00681	-0.00617	-0.00632
	tot	-0.01224	-0.01063	-0.01079	-0.00998	-0.00961	-0.00879
30	c	-0.00001	-0.00001	-0.00001	-0.00001	-0.00001	-0.00001
	tr1	-0.00329	-0.00336	-0.00390	-0.00210	-0.00239	-0.00140
	tr2	-0.00734	-0.00566	-0.00530	-0.00608	-0.00541	-0.00549
	tot	-0.01064	-0.00903	-0.00921	-0.00818	-0.00781	-0.00690
35	c	-0.00001	-0.00001	-0.00001	-0.00001	-0.00001	-0.00001
	tr1	-0.00222	-0.00234	-0.00289	-0.00103	-0.00133	-0.00034
	tr2	-0.00682	-0.00510	-0.00474	-0.00536	-0.00467	-0.00468
	tot	-0.00905	-0.00744	-0.00764	-0.00640	-0.00601	-0.00503
40	c	-0.00001	-0.00001	-0.00001	-0.00001	-0.00002	-0.00002
	tr1	-0.00114	-0.00131	-0.00187	0.00005	-0.00026	0.00074
	tr2	-0.00632	-0.00454	-0.00420	-0.00466	-0.00394	-0.00388
	tot	-0.00747	-0.00587	-0.00609	-0.00462	-0.00422	-0.00316
45	c	-0.00001	-0.00002	-0.00002	-0.00002	-0.00002	-0.00002
	tr1	-0.00006	-0.00028	-0.00085	0.00113	0.00081	0.00183
	tr2	-0.00583	-0.00401	-0.00367	-0.00397	-0.00323	-0.00310
	tot	-0.00590	-0.00430	-0.00454	-0.00285	-0.00244	-0.00129
50	c	-0.00002	-0.00002	-0.00002	-0.00002	-0.00003	-0.00003
	tr1	0.00104	0.00076	0.00017	0.00223	0.00190	0.00293
	tr2	-0.00535	-0.00349	-0.00316	-0.00330	-0.00254	-0.00234
	tot	-0.00433	-0.00274	-0.00301	-0.00109	-0.00066	0.00057
55	c	-0.00002	-0.00003	-0.00003	-0.00003	-0.00003	-0.00003
	tr1	0.00214	0.00181	0.00120	0.00335	0.00300	0.00405
	tr2	-0.00489	-0.00298	-0.00267	-0.00265	-0.00186	-0.00159
	tot	-0.00278	-0.00120	-0.00150	0.00067	0.00111	0.00243
60	c	-0.00003	-0.00003	-0.00003	-0.00003	-0.00004	-0.00004
	tr1	0.00325	0.00287	0.00224	0.00448	0.00412	0.00519
	tr2	-0.00445	-0.00250	-0.00220	-0.00201	-0.00120	-0.00087
	tot	-0.00123	0.00034	0.00001	0.00243	0.00288	0.00429
65	c	-0.00003	-0.00004	-0.00004	-0.00004	-0.00004	-0.00004
	tr1	0.00437	0.00394	0.00329	0.00562	0.00525	0.00635
	tr2	-0.00403	-0.00203	-0.00174	-0.00140	-0.00057	-0.00016
	tot	0.00031	0.00187	0.00151	0.00418	0.00464	0.00614
70	c	-0.00004	-0.00004	-0.00004	-0.00005	-0.00005	-0.00005
	tr1	0.00550	0.00502	0.00434	0.00679	0.00641	0.00753
	tr2	-0.00363	-0.00159	-0.00131	-0.00080	0.00005	0.00053
	tot	0.00183	0.00339	0.00299	0.00594	0.00641	0.00801
75	c	-0.00004	-0.00005	-0.00005	-0.00005	-0.00006	-0.00006
	tr1	0.00665	0.00611	0.00541	0.00798	0.00758	0.00874
	tr2	-0.00325	-0.00117	-0.00090	-0.00023	0.00065	0.00119
	tot	0.00335	0.00490	0.00446	0.00769	0.00817	0.00987
80	c	-0.00005	-0.00005	-0.00005	-0.00006	-0.00006	-0.00006
	tr1	0.00781	0.00722	0.00650	0.00919	0.00878	0.00997
	tr2	-0.00290	-0.00077	-0.00051	0.00032	0.00122	0.00183
	tot	0.00486	0.00640	0.00593	0.00944	0.00994	0.01174
85	c	-0.00005	-0.00006	-0.00006	-0.00007	-0.00007	-0.00007
	tr1	0.00898	0.00835	0.00759	0.01042	0.01001	0.01124
	tr2	-0.00257	-0.00039	-0.00015	0.00084	0.00176	0.00245
	tot	0.00637	0.00790	0.00738	0.01120	0.01171	0.01362
90	c	-0.00006	-0.00006	-0.00007	-0.00007	-0.00008	-0.00008
	tr1	0.01018	0.00949	0.00871	0.01169	0.01127	0.01254
	tr2	-0.00226	-0.00004	0.00019	0.00134	0.00229	0.00305
	tot	0.00786	0.00939	0.00883	0.01296	0.01348	0.01551
95	c	-0.00006	-0.00007	-0.00007	-0.00008	-0.00008	-0.00009
	tr1	0.01139	0.01066	0.00984	0.01299	0.01256	0.01388
	tr2	-0.00198	0.00029	0.00050	0.00181	0.00278	0.00362
	tot	0.00935	0.01087	0.01026	0.01472	0.01526	0.01740
100	c	-0.00007	-0.00008	-0.00008	-0.00009	-0.00009	-0.00010
	tr1	0.01263	0.01185	0.01099	0.01432	0.01388	0.01525
	tr2	-0.00173	0.00058	0.00078	0.00226	0.00325	0.00416
	tot	0.01082	0.01235	0.01169	0.01649	0.01704	0.01931

TABLE VI. The higher-order nuclear recoil correction for the  $4s$ ,  $5s$ ,  $5p$ , and  $5d$  states in terms of the function  $F$  defined by Eq. (35). The column labeled  $\langle\psi_v|\tilde{h}_{\text{h.o.}}^{\text{NMS}}|\psi_v\rangle$  denotes the results obtained by means of the model QED operator,  $\langle\psi_v|V_{\text{s.l.}}|\psi_v\rangle$  is the contribution of the semilocal part of the model operator, and “Exact” stands for the *ab initio* values. The  $ns$  states with  $n \leq 3$  and the  $np$  and  $nd$  states with  $n \leq 4$  are omitted since the operator  $\tilde{h}_{\text{h.o.}}^{\text{NMS}}$  exactly reproduces the corresponding correction for them by construction.

$Z$	State	$\langle\psi_v V_{\text{s.l.}} \psi_v\rangle$	$\langle\psi_v \tilde{h}_{\text{h.o.}}^{\text{NMS}} \psi_v\rangle$	Exact	$Z$	State	$\langle\psi_v V_{\text{s.l.}} \psi_v\rangle$	$\langle\psi_v \tilde{h}_{\text{h.o.}}^{\text{NMS}} \psi_v\rangle$	Exact
10	$4s$	1.2024	1.5325	1.5295	60	$4s$	0.8494	1.4804	1.4767
	$5s$	1.2017	1.5445	1.5397		$5s$	0.8394	1.4833	1.4772
	$5p_{1/2}$	-0.0922	-0.0545	-0.0558		$5p_{1/2}$	0.1282	0.1782	0.1765
	$5p_{3/2}$	-0.0965	-0.0590	-0.0603		$5p_{3/2}$	0.0221	0.0540	0.0517
	$5d_{3/2}$	-0.0279	-0.0157	-0.0145		$5d_{3/2}$	-0.0010	0.0058	0.0053
	$5d_{5/2}$	-0.0278	-0.0156	-0.0145		$5d_{5/2}$	-0.0019	0.0044	0.0043
20	$4s$	1.0162	1.3896	1.3865	70	$4s$	0.9227	1.6503	1.6463
	$5s$	1.0141	1.4010	1.3960		$5s$	0.9088	1.6475	1.6409
	$5p_{1/2}$	-0.0555	-0.0204	-0.0218		$5p_{1/2}$	0.1963	0.2652	0.2634
	$5p_{3/2}$	-0.0692	-0.0349	-0.0363		$5p_{3/2}$	0.0406	0.0762	0.0736
	$5d_{3/2}$	-0.0225	-0.0116	-0.0107		$5d_{3/2}$	0.0047	0.0110	0.0101
	$5d_{5/2}$	-0.0224	-0.0116	-0.0107		$5d_{5/2}$	0.0028	0.0084	0.0080
30	$4s$	0.9090	1.3357	1.3325	80	$4s$	1.0683	1.9249	1.9205
	$5s$	0.9053	1.3460	1.3408		$5s$	1.0478	1.9125	1.9055
	$5p_{1/2}$	-0.0162	0.0177	0.0162		$5p_{1/2}$	0.2880	0.3904	0.3885
	$5p_{3/2}$	-0.0437	-0.0119	-0.0136		$5p_{3/2}$	0.0578	0.0990	0.0961
	$5d_{3/2}$	-0.0172	-0.0075	-0.0069		$5d_{3/2}$	0.0108	0.0169	0.0156
	$5d_{5/2}$	-0.0171	-0.0076	-0.0069		$5d_{5/2}$	0.0073	0.0124	0.0117
40	$4s$	0.8484	1.3348	1.3314	90	$4s$	1.3278	2.3698	2.3650
	$5s$	0.8430	1.3436	1.3381		$5s$	1.2952	2.3406	2.3329
	$5p_{1/2}$	0.0262	0.0612	0.0596		$5p_{1/2}$	0.4244	0.5875	0.5855
	$5p_{3/2}$	-0.0200	0.0103	0.0084		$5p_{3/2}$	0.0739	0.1228	0.1195
	$5d_{3/2}$	-0.0119	-0.0033	-0.0031		$5d_{3/2}$	0.0173	0.0236	0.0220
	$5d_{5/2}$	-0.0119	-0.0036	-0.0032		$5d_{5/2}$	0.0117	0.0165	0.0155
50	$4s$	0.8280	1.3813	1.3777	100	$4s$	1.7885	3.1190	3.1142
	$5s$	0.8206	1.3877	1.3820		$5s$	1.7322	3.0568	3.0496
	$5p_{1/2}$	0.0733	0.1131	0.1115		$5p_{1/2}$	0.6515	0.9319	0.9297
	$5p_{3/2}$	0.0019	0.0322	0.0301		$5p_{3/2}$	0.0889	0.1478	0.1444
	$5d_{3/2}$	-0.0065	0.0011	0.0010		$5d_{3/2}$	0.0246	0.0317	0.0297
	$5d_{5/2}$	-0.0068	0.0004	0.0006		$5d_{5/2}$	0.0158	0.0206	0.0193

TABLE VII. The one-electron nuclear recoil correction beyond the Breit approximation for the valence  $ns$  electron in neutral alkali metals in terms of the function  $F$  defined by Eq. (35). The labels CH and  $x_\alpha = 0, 1/3, 2/3$ , and 1 correspond to the different effective potentials. See the text for details.

Atom	Approach	CH	$x_\alpha = 0$	$x_\alpha = 1/3$	$x_\alpha = 2/3$	$x_\alpha = 1$
Na $3s$	$\langle \psi_v   V_{s.l.}   \psi_v \rangle$	0.0502	0.0446	0.0437	0.0473	0.0575
	$\langle \psi_v   \tilde{h}_{h.o.}^{NMS}   \psi_v \rangle$	0.0581	0.0516	0.0508	0.0553	0.0676
	Exact	0.0561	0.0499	0.0496	0.0544	0.0671
K $4s$	$\langle \psi_v   V_{s.l.}   \psi_v \rangle$	0.0255	0.0214	0.0213	0.0243	0.0319
	$\langle \psi_v   \tilde{h}_{h.o.}^{NMS}   \psi_v \rangle$	0.0313	0.0263	0.0264	0.0302	0.0400
	Exact	0.0311	0.0261	0.0263	0.0302	0.0401
Rb $5s$	$\langle \psi_v   V_{s.l.}   \psi_v \rangle$	0.0100	0.0080	0.0082	0.0098	0.0136
	$\langle \psi_v   \tilde{h}_{h.o.}^{NMS}   \psi_v \rangle$	0.0141	0.0112	0.0116	0.0140	0.0195
	Exact	0.0142	0.0113	0.0117	0.0141	0.0197
Cs $6s$	$\langle \psi_v   V_{s.l.}   \psi_v \rangle$	0.00645	0.00504	0.00525	0.00642	0.00927
	$\langle \psi_v   \tilde{h}_{h.o.}^{NMS}   \psi_v \rangle$	0.01019	0.00796	0.00835	0.01026	0.01490
	Exact	0.01028	0.00803	0.00841	0.01034	0.01500
Fr $7s$	$\langle \psi_v   V_{s.l.}   \psi_v \rangle$	0.00586	0.00416	0.00457	0.00595	0.00906
	$\langle \psi_v   \tilde{h}_{h.o.}^{NMS}   \psi_v \rangle$	0.00999	0.00708	0.00782	0.01022	0.01563
	Exact	0.01004	0.00712	0.00786	0.01026	0.01568

the operator exactly reproduces the QED recoil contributions for these states. For this reason, the “predictive power” of the operator can be tested by applying it to evaluation of the corresponding corrections for the states with higher values of the principal quantum number. In Table VI, the nuclear recoil contributions beyond the Breit approximation are given for the  $4s$ ,  $5s$ ,  $5p_{1/2}$ ,  $5p_{3/2}$ ,  $5d_{3/2}$ , and  $5d_{5/2}$  states in hydrogenlike ions. The columns labeled  $\langle \psi_v | V_{s.l.} | \psi_v \rangle$  and  $\langle \psi_v | \tilde{h}_{h.o.}^{NMS} | \psi_v \rangle$  contain the predictions obtained using the semilocal part (29) of the model-QED operator and the total model-QED operator (28), respectively. These values are compared with the *ab initio* results taken from Tables I-V and shown in the last column. As one can see, there is generally good agreement between the data, especially for the  $s$  states. We stress the importance of the nonlocal part of the model-QED operator. For the  $np$  and  $nd$  states the functions  $F_{n_i n_k}$  change the sign for the middle values of  $Z$  and, accordingly, have small absolute values there. As a result, the relative accuracy of the model-QED-operator predictions slightly decreases in these regions.

To date, the QED contribution to the NMS in many-electron systems was usually evaluated within the independent-electron approximation by performing the calculations in the extended Furry picture, see, e.g., Refs. [4, 10, 84]. To demonstrate the performance of the developed model-QED-operator approach, we apply it to evaluation of the nuclear recoil effect on valence-electron energies in neutral alkali metals. First, we perform *ab initio* calculations of the one-electron contribution for the  $ns$  states by using a local effective potential as  $V$  in Eq. (5). We use the core-Hartree (CH) and  $x_\alpha$  potentials, which are discussed in Appendix C. The results of *ab initio* calculations of the QED contribution to the NMS are presented in Table VII in rows labeled “Exact”. The model-QED-operator values are obtained by averaging the operator (28) with the valence-electron wave functions determined from the Dirac equation (5), in which the potential  $V$  is given by Eq. (C3). Along with the total model-operator predictions,  $\langle \psi_v | \tilde{h}_{\text{h.o.}}^{\text{NMS}} | \psi_v \rangle$ , the results  $\langle \psi_v | V_{\text{s.l.}} | \psi_v \rangle$  for the semilocal part (29) only are shown as well. As it is seen from Table VII, for all the alkali metals there is good agreement between the approximate and exact values. Therefore, the model-QED operator based on the calculations for hydrogenlike ions works also reasonably well in the nonhydrogenic cases.

To conclude the discussion of alkali metals, let us note that, as in Ref. [122], the strong dependence of the final results on the choice of the potential for the initial approximation takes place. The scatter of the results is related obviously with the approximate treatment of the interelectronic-interaction effects. We believe that the developed model-QED operator for the nuclear recoil effect merged with the standard methods to treat the electron correlations will make it possible to perform much more accurate evaluation. However, such calculations are out of the scope of the present work. We reserve systematic calculations with the model-QED operator for the nuclear recoil effect for future research.

## V. CONCLUSION

In the present paper, we have worked out the model-QED-operator approach to treat the nuclear recoil effect on binding energies in many-electron atomic systems beyond the Breit approximation. The approach is similar to the one proposed earlier for approximate calculations of the radiative corrections to energy levels [46]. The developed operator can be readily included into any relativistic calculations based on the Dirac-Coulomb-Breit Hamiltonian.

The performance of the approach was demonstrated by comparing the model-QED-operator predictions with the results of the rigorous QED calculations.

## VI. ACKNOWLEDGEMENTS

The work was supported by the Foundation for the Advancement of Theoretical Physics and Mathematics “BASIS” and by RFBR and ROSATOM according to the research project No. 20-21-00098. The work of I.S.A. was supported by the German-Russian Interdisciplinary Science Center (G-RISC) funded by the German Federal Foreign Office via the German Academic Exchange Service (DAAD).

### Appendix A: One- and two-electron contributions to the nuclear recoil effect on binding energies of quasi-degenerate levels

In the present Appendix, we derive the fully relativistic expressions for the contributions of the nuclear recoil effect on binding energies within the two-time Green’s function (TTGF) method [96]. Let us denote the unperturbed wave functions of the two states under consideration as  $|u_i\rangle$  and  $|u_k\rangle$ . During the derivation, we assume that the unperturbed energies  $E_i^{(0)}$  and  $E_k^{(0)}$ , which corresponds to these states, differ and, therefore,  $|u_i\rangle \neq |u_k\rangle$ . However, all the obtained expressions are valid for the coinciding energies and, of course, boil down to the expressions (8) and (17) in the case of diagonal matrix elements. In order to derive the formulas, we introduce a model subspace  $\Omega$ , which is spanned by the states  $|u_i\rangle$  and  $|u_k\rangle$ , and construct for these states the QED perturbation theory as for quasi-degenerate levels. The projector on  $\Omega$  reads as

$$P^{(0)} = |u_i\rangle\langle u_i| + |u_k\rangle\langle u_k|. \quad (\text{A1})$$

The derivation procedure can be readily generalized for an arbitrary number of quasi-degenerate levels.

First, let us recall the basic ideas of the TTGF methods in the application to quasi-degenerate levels. The detailed description of the method can be found, e.g., in Refs. [96, 109, 126]. The  $N$ -electron TTGF is defined as

$$G(t', t; \mathbf{r}'_1, \dots, \mathbf{r}'_N; \mathbf{r}_1, \dots, \mathbf{r}_N) = \langle 0 | T \psi(x'_1) \cdots \psi(x'_N) \bar{\psi}(x_N) \cdots \bar{\psi}(x_1) | 0 \rangle \Bigg|_{\substack{t'_1 = \dots = t'_N \equiv t' \\ t_1 = \dots = t_N \equiv t}}, \quad (\text{A2})$$



where  $\psi$  is the electron-positron field operator in the Heisenberg representation,  $\bar{\psi} = \psi^\dagger \gamma^0$ ,  $x = (t^0, \mathbf{r})$ , and  $T$  is the time-ordering operator. Turning to the mixed representation, one obtains

$$\begin{aligned} & \mathcal{G}(E; \mathbf{r}'_1, \dots, \mathbf{r}'_N; \mathbf{r}_1, \dots, \mathbf{r}_N) \delta(E - E') \\ &= \frac{1}{2\pi i} \frac{1}{N!} \int_{-\infty}^{\infty} dt dt' e^{iE't' - iEt} G(t', t; \mathbf{r}'_1, \dots, \mathbf{r}'_N; \mathbf{r}_1, \dots, \mathbf{r}_N). \end{aligned} \quad (\text{A3})$$

Employing  $P^{(0)}$ , we can introduce the projection of the Green's function (A3) on the subspace  $\Omega$ ,

$$g(E) = P^{(0)} \mathcal{G}(E) \gamma_1^0 \dots \gamma_N^0 P^{(0)}, \quad (\text{A4})$$

and then determine the  $\hat{K}$  and  $\hat{P}$  operators:

$$\hat{K} \equiv \frac{1}{2\pi i} \oint_{\Gamma} dE E g(E), \quad (\text{A5})$$

$$\hat{P} \equiv \frac{1}{2\pi i} \oint_{\Gamma} dE g(E). \quad (\text{A6})$$

The anticlockwise oriented contour  $\Gamma$  in the complex  $E$  plane surrounds the poles corresponding to the quasi-degenerate levels and keeps outside all other singularities of  $g(E)$ .

The investigated system is fully described by the effective operator  $\hat{H}$  defined as

$$\hat{H} = \hat{P}^{-1/2} \hat{K} \hat{P}^{-1/2}. \quad (\text{A7})$$

The perturbation theory for the Green's function (A2) leads to the perturbation series for the operator  $\hat{H}$ .

To first order in  $m/M$ , the nuclear recoil effect is described by the one- and two-electron Feynman diagrams depicted in Figs. 1 and 2. The Feynman rules for these diagrams are formulated, e.g., in Ref. [26], see also Ref. [96]. The first-order contribution to the operator  $\hat{H}$  can be expressed as

$$\hat{H}^{(1)} = \hat{K}^{(1)} - \frac{1}{2} \hat{P}^{(1)} \hat{K}^{(0)} - \frac{1}{2} \hat{K}^{(0)} \hat{P}^{(1)}, \quad (\text{A8})$$

where the superscripts denote the orders in the expansion parameter. The contributions of the nuclear recoil effect are determined by the matrix elements of the operator (A8) in the basis of the unperturbed functions  $|u_i\rangle$  and  $|u_k\rangle$ :

$$H_{ik}^{(1)} \equiv \langle u_i | \hat{H}^{(1)} | u_k \rangle. \quad (\text{A9})$$

To zeroth order, the matrix of the operator  $\hat{K}$  is diagonal,  $K_{ik}^{(0)} = E_i^{(0)} \delta_{ik}$ . Therefore, one can obtain

$$H_{ik}^{(1)} = K_{ik}^{(1)} - \frac{E_i^{(0)} + E_k^{(0)}}{2} P_{ik}^{(1)}. \quad (\text{A10})$$

Let us now directly turn to the derivation of the desired nonperturbative (in  $\alpha Z$ ) formulas for the nuclear recoil effect on binding energies. We start from the one-electron (NMS) contribution corresponding to the diagrams in Fig. 1. In this case,  $N = 1$  and the unperturbed wave functions  $|u_i\rangle$ ,  $|u_k\rangle$  and energies  $E_i^{(0)}$ ,  $E_k^{(0)}$  are given by the Dirac eigenfunctions and eigenvalues, respectively, see Eq. (5). The present derivation is similar to the one for the self-energy diagram shown in Fig. 3. Employing the Feynman rules [26], one can obtain the following expression for the matrix element of the Green's function  $\Delta g_{\text{NMS}}^{(1)}(E)$  projected on the subspace  $\Omega$  [96]:

$$\Delta g_{\text{NMS},ik}^{(1)}(E) = \frac{\langle \psi_i | P(E) | \psi_k \rangle}{(E - \varepsilon_i)(E - \varepsilon_k)}, \quad (\text{A11})$$

where the operator  $P$  is defined in Eq. (9). The corresponding contributions to the  $\hat{K}$  and  $\hat{P}$  operators read as:

$$K_{\text{NMS},ik}^{(1)} = \frac{1}{2\pi i} \oint_{\Gamma} dE E \Delta g_{\text{NMS},ik}^{(1)}(E) = \frac{\varepsilon_i}{\varepsilon_i - \varepsilon_k} \langle \psi_i | P(\varepsilon_i) | \psi_k \rangle + \frac{\varepsilon_k}{\varepsilon_k - \varepsilon_i} \langle \psi_i | P(\varepsilon_k) | \psi_k \rangle, \quad (\text{A12})$$

$$P_{\text{NMS},ik}^{(1)} = \frac{1}{2\pi i} \oint_{\Gamma} dE \Delta g_{\text{NMS},ik}^{(1)}(E) = \frac{1}{\varepsilon_i - \varepsilon_k} \langle \psi_i | P(\varepsilon_i) | \psi_k \rangle + \frac{1}{\varepsilon_k - \varepsilon_i} \langle \psi_i | P(\varepsilon_k) | \psi_k \rangle. \quad (\text{A13})$$

Substituting Eqs. (A12) and (A13) into the formula (A10), one finally obtains the NMS contribution

$$H_{\text{NMS},ik} = \frac{1}{2} \left[ \langle \psi_i | P(\varepsilon_i) | \psi_k \rangle + \langle \psi_i | P(\varepsilon_k) | \psi_k \rangle \right]. \quad (\text{A14})$$

The derivation of the nonperturbative (in  $\alpha Z$ ) expression for the two-electron (SMS) contribution in Fig. 2 is also straightforward but more tedious. In this case,  $N = 2$  and we, for simplicity, assume that the unperturbed wave functions  $|u_i\rangle$  and  $|u_k\rangle$  are given by the one-determinant wave functions  $\Psi_{i_1 i_2}$  and  $\Psi_{k_1 k_2}$ , respectively, see Eq. (16). The corresponding unperturbed energies are equal to  $E_i^{(0)} = \varepsilon_{i_1} + \varepsilon_{i_2}$  and  $E_k^{(0)} = \varepsilon_{k_1} + \varepsilon_{k_2}$ . The derivation repeats the one for the one-photon-exchange diagram in Fig. 5. The Green's

function  $\Delta g_{\text{SMS}}^{(1)}(E)$  projected on the subspace  $\Omega$  can be written as [26, 96]

$$\begin{aligned} \Delta g_{\text{SMS},ik}^{(1)}(E) &= \left(\frac{i}{2\pi}\right)^2 \int dp_1 dp'_1 \sum_P (-1)^P \langle \psi_{P_{i_1}} \psi_{P_{i_2}} | R(p_1 - p'_1) | \psi_{k_1} \psi_{k_2} \rangle \\ &\times \frac{1}{(p'_1 - \varepsilon_{P_{i_1}} + i0)(E - p'_1 - \varepsilon_{P_{i_2}} + i0)} \frac{1}{(p_1 - \varepsilon_{k_1} + i0)(E - p_1 - \varepsilon_{k_2} + i0)}, \end{aligned} \quad (\text{A15})$$

where the operator  $R$  is defined by Eq. (10). Using the identity

$$\frac{1}{(p'_1 - \varepsilon_{P_{i_1}} + i0)(E - p'_1 - \varepsilon_{P_{i_2}} + i0)} = \frac{1}{E - E_i^{(0)}} \left( \frac{1}{p'_1 - \varepsilon_{P_{i_1}} + i0} + \frac{1}{E - p'_1 - \varepsilon_{P_{i_2}} + i0} \right) \quad (\text{A16})$$

and a similar one for the second pair of denominators in Eq. (A15), one can explicitly separate the poles of the Green's function located inside the contour  $\Gamma$ . Then, the contribution to the  $\hat{K}$  operator is

$$\begin{aligned} K_{\text{SMS},ik}^{(1)} &= \oint_{\Gamma} dE E \Delta g_{\text{SMS},ik}^{(1)}(E) \\ &= \left(\frac{i}{2\pi}\right)^2 \int dp_1 dp'_1 \sum_P (-1)^P \langle \psi_{P_{i_1}} \psi_{P_{i_2}} | R(p_1 - p'_1) | \psi_{k_1} \psi_{k_2} \rangle \\ &\times \left\{ \frac{E_i^{(0)}}{E_i^{(0)} - E_k^{(0)}} \left( \frac{2\pi}{i} \delta(p'_1 - \varepsilon_{P_{i_1}}) \right) \left( \frac{1}{p_1 - \varepsilon_{k_1} + i0} + \frac{1}{E_i^{(0)} - p_1 - \varepsilon_{k_2} + i0} \right) \right. \\ &\left. + \frac{E_k^{(0)}}{E_k^{(0)} - E_i^{(0)}} \left( \frac{1}{p'_1 - \varepsilon_{P_{i_1}} + i0} + \frac{1}{E_k^{(0)} - p'_1 - \varepsilon_{P_{i_2}} + i0} \right) \left( \frac{2\pi}{i} \delta(p_1 - \varepsilon_{k_1}) \right) \right\}, \end{aligned} \quad (\text{A17})$$

where the identity

$$\frac{1}{p - \varepsilon + i0} + \frac{1}{-p + \varepsilon + i0} = \frac{2\pi}{i} \delta(p - \varepsilon) \quad (\text{A18})$$

was employed. Defining the coefficients  $A$  and  $B$  so that  $K_{\text{SMS},ik}^{(1)} \equiv AE_i^{(0)} + BE_k^{(0)}$ , the contribution to the operator  $\hat{P}$  can be expressed as  $P_{\text{SMS},ik}^{(1)} = A + B$ . Therefore, the formula (A10)

results in

$$\begin{aligned}
H_{\text{SMS},ik} &= \frac{1}{2} \frac{i}{2\pi} \int d\omega \sum_P (-1)^P \\
&\times \left\{ \langle \psi_{P_{i_1}} \psi_{P_{i_2}} | R(\omega - \varepsilon_{P_{i_1}}) | \psi_{k_1} \psi_{k_2} \rangle \left( \frac{1}{\omega - \varepsilon_{k_1} + i0} + \frac{1}{E_i^{(0)} - \omega - \varepsilon_{k_2} + i0} \right) \right. \\
&\quad \left. + \langle \psi_{P_{i_1}} \psi_{P_{i_2}} | R(\varepsilon_{k_1} - \omega) | \psi_{k_1} \psi_{k_2} \rangle \left( \frac{1}{\omega - \varepsilon_{P_{i_1}} + i0} + \frac{1}{E_k^{(0)} - \omega - \varepsilon_{P_{i_2}} + i0} \right) \right\}.
\end{aligned} \tag{A19}$$

The integration over  $\omega$  can be performed using the standard identity ( $\omega_1 < 0 < \omega_2$ ):

$$\int_{\omega_1}^{\omega_2} d\omega \frac{f(\omega)}{\omega \pm i0} = \mp i\pi f(0) + \text{P.V.} \int_{\omega_1}^{\omega_2} d\omega \frac{f(\omega)}{\omega}, \tag{A20}$$

where P.V means the principal-value integral. Indeed, applying the formula (A20) to all four terms in Eq. (A19) and taking into account that all the principal-value integrals vanish due to the fact that  $R(\omega)$  is the even function of  $\omega$ , one finally obtains the SMS contribution

$$H_{\text{SMS},ik} = \frac{1}{2} \sum_P (-1)^P \left[ \langle \psi_{P_{i_1}} \psi_{P_{i_2}} | R(\Delta_1) | \psi_{k_1} \psi_{k_2} \rangle + \langle \psi_{P_{i_1}} \psi_{P_{i_2}} | R(\Delta_2) | \psi_{k_1} \psi_{k_2} \rangle \right], \tag{A21}$$

where  $\Delta_1 = \varepsilon_{P_{i_1}} - \varepsilon_{k_1}$  and  $\Delta_2 = \varepsilon_{P_{i_2}} - \varepsilon_{k_2}$ .

## Appendix B: Computational formulas for the one-electron contributions

In view of the definition (9), the expression (A14) obtained in Appendix A is given in a form that allows one to use the finite-basis-set methods [120, 121, 127] for its calculations. Therefore, the main difficulty is related with the evaluation of the integral over  $\omega$ . For large real values of  $\omega$ , the photon propagator (7) is a strongly oscillating function. It is convenient to perform the Wick's rotation to overcome this obstacle. In the present Appendix, we discuss the related transformations for the contribution  $H_{\text{NMS},ik}$ .

Employing Eq. (12), one can represent Eq. (A14) as the sum of the Coulomb, one-transverse-photon, and two-transverse-photon contributions

$$H_{\text{NMS},ik} = H_{\text{NMS},ik}^c + H_{\text{NMS},ik}^{\text{tr1}} + H_{\text{NMS},ik}^{\text{tr2}}. \tag{B1}$$

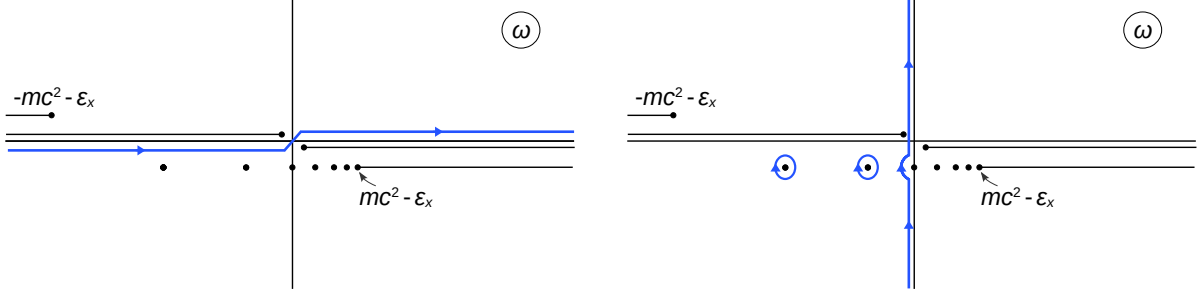


FIG. 6. The poles and the branch cuts of the integrand in the operator  $P(\varepsilon_x)$  for the one- and two-transverse-photon contributions. The integration contour: the original one oriented along the real axis (left panel); the rotated to the imaginary one (right panel).

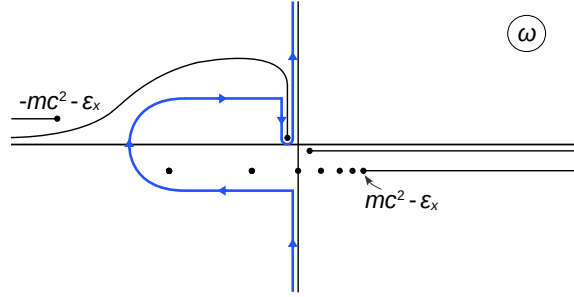


FIG. 7. The poles and the branch cuts of the integrand in the operator  $P(\varepsilon_x)$  for the one- and two-transverse-photon contributions. The integration contour in the complex plane is chosen to avoid all the singularities of the integrand.

In the Coulomb contribution, the integration over  $\omega$  can be performed analytically by means of the identity (A20)

$$H_{\text{NMS},ik}^c = \frac{1}{2} \left[ \sum_n^{\varepsilon_n > 0} \langle \psi_i \psi_n | R_c | \psi_n \psi_k \rangle - \sum_n^{\varepsilon_n < 0} \langle \psi_i \psi_n | R_c | \psi_n \psi_k \rangle \right]. \quad (\text{B2})$$

The one- and two-transverse-photon contributions are handled identically. In what follows in this Appendix, we will refer to them together as the “transverse-photon” (tr) ones. In the left panel of Fig. 6, the original integration contour oriented along the real axis is shown. The poles and the branch cuts of the integrand are presented as well. Upon the Wick’s rotation to the imaginary axis, the bound-state poles of the electron Green’s function are picked up as the residues, see the right panel in Fig. 6. The final formulas for the transverse-photon

contribution can be written as a sum of three terms

$$H_{\text{NMS},ik}^{\text{tr}} = H_{\text{NMS},ik}^{\text{tr}(a)} + H_{\text{NMS},ik}^{\text{tr}(b)} + H_{\text{NMS},ik}^{\text{tr}(c)}. \quad (\text{B3})$$

The first term arises from the residues shown by the circles in Fig. 6 and reads as

$$H_{\text{NMS},ik}^{\text{tr}(a)} = \frac{1}{2} \sum_{x=i,k} \sum_n^{-1 < \varepsilon_n < \varepsilon_x} \langle \psi_i \psi_n | R_{\text{tr}}(\varepsilon_n - \varepsilon_x) | \psi_n \psi_k \rangle, \quad (\text{B4})$$

where for brevity we have introduced the summation over  $x$  in order to take into account the symmetric form of the expression with respect to the argument of  $P(E)$ . The second term corresponds to the case of degeneracy between the states of the opposite parity. This term originates from the poles located at  $\omega = 0$  and has the form

$$H_{\text{NMS},ik}^{\text{tr}(b)} = \frac{1}{4} \sum_{x=i,k} \sum_n^{\varepsilon_n = \varepsilon_x} \langle \psi_i \psi_n | R_{\text{tr}}(0) | \psi_n \psi_k \rangle. \quad (\text{B5})$$

Finally, the third term corresponds to the integration over the imaginary axis

$$H_{\text{NMS},ik}^{\text{tr}(c)} = \frac{1}{2} \sum_{x=i,k} \sum_n^{\varepsilon_n \neq \varepsilon_x} \frac{1}{\pi} \int_0^\infty dy \frac{\varepsilon_n - \varepsilon_x}{y^2 + (\varepsilon_n - \varepsilon_x)^2} \langle \psi_i \psi_n | R_{\text{tr}}(iy) | \psi_n \psi_k \rangle. \quad (\text{B6})$$

The expressions similar to (B2), (B4), (B5), and (B6) were derived, e.g., in Ref. [32]. However, only the case of the diagonal matrix elements was considered. Moreover, in Ref. [32] the formulas for the higher-order QED corrections beyond the Breit approximation were given, while the present ones include the lowest-relativistic contributions as well.

As an additional crosscheck of the  $\omega$ -integration routine, we perform it also by employing the contour schematically shown in Fig. 7. This contour is chosen to bypass all the singularities in the complex plane. The matrix elements  $H_{\text{NMS},ik}$  have been evaluated for both variants of the integration-contour rotation. The results are found to be in excellent agreement with each other.

### Appendix C: Local effective potentials

In Sec. IV, in order to test the performance of the model-QED operator for the nuclear recoil effect, we need substitute the core-Hartree (CH) and  $x_\alpha$  potentials (see, e.g., Ref. [122]) instead of  $V$  in Eq. (5). These potentials can be expressed via the charge densities of the valence electron,

$$\rho_v(r) = g_v^2(r) + f_v^2(r), \quad (\text{C1})$$

and the core,

$$\rho_{\text{core}}(r) = \sum_c (2j_c + 1) \left[ g_c^2(r) + f_c^2(r) \right]. \quad (\text{C2})$$

Here the large,  $g$ , and small,  $f$ , components of the Dirac wave function in Eqs. (C1) and (C2) are determined self-consistently in the local potential

$$V(r) = -\frac{\alpha Z_{\text{eff}}(r)}{r}, \quad (\text{C3})$$

where  $Z_{\text{eff}}(r)$  is the effective charge. The CH potential is given by

$$Z_{\text{eff}}^{\text{CH}}(r) = Z_{\text{nucl}}(r) - r \int_0^{\infty} dr' \frac{\rho_{\text{core}}(r')}{\max\{r, r'\}}, \quad (\text{C4})$$

where  $Z_{\text{nucl}}(r)$  accounts for the finite size of the nucleus. Defining the total charge density,  $\rho_{\text{tot}} = \rho_{\text{core}} + \rho_v$ , the effective charge for the  $x_\alpha$  potentials can be written in the form

$$Z_{\text{eff}}^{x_\alpha}(r) = Z_{\text{nucl}}(r) - r \int_0^{\infty} dr' \frac{\rho_{\text{tot}}(r')}{\max\{r, r'\}} + x_\alpha \left[ \frac{81}{32\pi^2} r \rho_{\text{tot}}(r) \right]^{1/3}. \quad (\text{C5})$$

We use the values of  $x_\alpha$  equal to 0, 1/3, 2/3, and 1. The choice  $x_\alpha = 0$  leads to the Dirac-Hartree potential,  $x_\alpha = 2/3$  corresponds to the Kohn-Sham potential [123], while  $x_\alpha = 1$  is the Dirac-Slater potential [124]. In order to restore the proper asymptotic behavior of the  $x_\alpha$  potentials, we introduce the Latter correction [125].

- 
- [1] S. R. Elliott, P. Beiersdorfer, and M. H. Chen, Phys. Rev. Lett. **76**, 1031 (1996); **77**, 4278(E) (1996).
  - [2] S. R. Elliott, P. Beiersdorfer, M. H. Chen, V. Decaux, and D. A. Knapp, Phys. Rev. C **57**, 583 (1998).
  - [3] R. Schuch, E. Lindroth, S. Madzunkov, M. Fogle, T. Mohamed, and P. Indelicato, Phys. Rev. Lett. **95**, 183003 (2005).
  - [4] R. Soria Orts, Z. Harman, J. R. Crespo López-Urrutia, A. N. Artemyev, H. Bruhns, A. J. G. Martínez, U. D. Jentschura, C. H. Keitel, A. Lapierre, V. Mironov, V. M. Shabaev, H. Tawara, I. I. Tupitsyn, J. Ullrich, and A. V. Volotka, Phys. Rev. Lett. **97**, 103002 (2006).

- [5] C. Brandau, C. Kozhuharov, Z. Harman, A. Müller, S. Schippers, Y. S. Kozhedub, D. Bernhard, S. Böhm, J. Jacobi, E. W. Schmidt, P. H. Mokler, F. Bosch, H.-J. Kluge, Th. Stöhlker, K. Beckert, P. Beller, F. Nolden, M. Steck, A. Gumberidze, R. Reuschl, U. Spillmann, F. J. Currell, I. I. Tupitsyn, V. M. Shabaev, U. D. Jentschura, C. H. Keitel, A. Wolf, and Z. Stachura, *Phys. Rev. Lett.* **100**, 073201 (2008).
- [6] F. Köhler, K. Blaum, M. Block, S. Chenmarev, S. Eliseev, D. A. Glazov, M. Goncharov, J. Hou, A. Kracke, D. A. Nesterenko, Y. N. Novikov, W. Quint, E. M. Ramirez, V. M. Shabaev, S. Sturm, A. V. Volotka, and G. Werth, *Nat. Commun.* **7**, 10246 (2016).
- [7] B. Maaß, T. Hüther, K. König, J. Krämer, J. Krause, A. Lovato, P. Müller, K. Pachucki, M. Puchalski, R. Roth, R. Sánchez, F. Sommer, R. B. Wiringa, and W. Nörtershäuser, *Phys. Rev. Lett.* **122**, 182501 (2019).
- [8] Á. Koszorús, X. F. Yang, W. G. Jiang, S. J. Novario, S. W. Bai, J. Billowes, C. L. Binnersley, M. L. Bissell, T. E. Cocolios, B. S. Cooper, R. P. de Groote, A. Ekström, K. T. Flanagan, C. Forssén, S. Franchoo, R. F. G. Ruiz, F. P. Gustafsson, G. Hagen, G. R. Jansen, A. Kanelakopoulos, M. Kortelainen, W. Nazarewicz, G. Neyens, T. Papenbrock, P.-G. Reinhard, C. M. Ricketts, B. K. Sahoo, A. R. Vernon, and S. G. Wilkins, *Nat. Phys.* **17**, 439 (2021).
- [9] T. Sailer, V. Debierre, Z. Harman, F. Heiße, C. König, J. Morgner, B. Tu, A. V. Volotka, C. H. Keitel, K. Blaum, and S. Sturm, *Nature* **606**, 479 (2022).
- [10] S. A. King, L. J. Spieß, P. Micke, A. Wilzewski, T. Leopold, E. Benkler, R. Lange, N. Huntemann, A. Surzhykov, V. A. Yerokhin, J. R. C. López-Urrutia, and P. O. Schmidt, *arXiv:2205.13053 [physics.atom-ph]* (2022).
- [11] J. Z. Han, C. Pan, K. Y. Zhang, X. F. Yang, S. Q. Zhang, J. C. Berengut, S. Goriely, H. Wang, Y. M. Yu, J. Meng, J. W. Zhang, and L. J. Wang, *Phys. Rev. Research* **4**, 033049 (2022).
- [12] C. Frugiuele, E. Fuchs, G. Perez, and M. Schlaffer, *Phys. Rev. D* **96**, 015011 (2017).
- [13] J. C. Berengut, D. Budker, C. Delaunay, V. V. Flambaum, C. Frugiuele, E. Fuchs, C. Grojean, R. Harnik, R. Ozeri, G. Perez, and Y. Soreq, *Phys. Rev. Lett.* **120**, 091801 (2018).
- [14] V. V. Flambaum, A. J. Geddes, and A. V. Viatkina, *Phys. Rev. A* **97**, 032510 (2018).
- [15] V. A. Yerokhin, R. A. Müller, A. Surzhykov, P. Micke, and P. O. Schmidt, *Phys. Rev. A* **101**, 012502 (2020).



- [16] N.-H. Rehbehn, M. K. Rosner, H. Bekker, J. C. Berengut, P. O. Schmidt, S. A. King, P. Micke, M. F. Gu, R. Müller, A. Surzhykov, and J. R. C. López-Urrutia, *Phys. Rev. A* **103**, L040801 (2021).
- [17] N. L. Figueroa, J. C. Berengut, V. A. Dzuba, V. V. Flambaum, D. Budker, and D. Antypas, *Phys. Rev. Lett.* **128**, 073001 (2022).
- [18] K. Ono, Y. Saito, T. Ishiyama, T. Higomoto, T. Takano, Y. Takasu, Y. Yamamoto, M. Tanaka, and Y. Takahashi, *Phys. Rev. X* **12**, 021033 (2022).
- [19] V. Debierre, C. H. Keitel, and Z. Harman, *Physics Letters B* **807**, 135527 (2020).
- [20] V. Debierre and N. S. Oreshkina, *Phys. Rev. A* **104**, 032825 (2021).
- [21] V. Debierre, C. H. Keitel, and Z. Harman, [arXiv:2202.01668](https://arxiv.org/abs/2202.01668) [physics.atom-ph] (2022), [arXiv:2202.01668](https://arxiv.org/abs/2202.01668).
- [22] V. Debierre, N. S. Oreshkina, I. A. Valuev, Z. Harman, and C. H. Keitel, [rXiv:2207.04868](https://arxiv.org/abs/2207.04868) [physics.atom-ph] (2022).
- [23] V. M. Shabaev, *Theor. Math. Phys.* **63**, 588 (1985), [*Teor. Mat. Fiz.* **63**, 394 (1985)].
- [24] V. M. Shabaev, *Sov. J. Nucl. Phys.* **47**, 69 (1988), [*Yad. Fiz.* **47**, 107 (1988)].
- [25] C. W. P. Palmer, *J. Phys. B: At. Mol. Phys.* **20**, 5987 (1987).
- [26] V. M. Shabaev, *Phys. Rev. A* **57**, 59 (1998).
- [27] K. Pachucki and H. Grotch, *Phys. Rev. A* **51**, 1854 (1995).
- [28] A. S. Yelkhovsky, e-print [hep-th/9403095](https://arxiv.org/abs/hep-th/9403095) (1994); *Zh. Eksp. Fiz.* **110**, 431 (1996).
- [29] G. S. Adkins, S. Morrison, and J. Sapirstein, *Phys. Rev. A* **76**, 042508 (2007).
- [30] V. A. Yerokhin and V. M. Shabaev, *Phys. Rev. Lett.* **115**, 233002 (2015).
- [31] V. A. Yerokhin and V. M. Shabaev, *Phys. Rev. A* **93**, 062514 (2016).
- [32] A. N. Artemyev, V. M. Shabaev, and V. A. Yerokhin, *Phys. Rev. A* **52**, 1884 (1995).
- [33] V. M. Shabaev, A. N. Artemyev, T. Beier, G. Plunien, V. A. Yerokhin, and G. Soff, *Phys. Rev. A* **57**, 4235 (1998).
- [34] A. V. Malyshev, R. V. Popov, V. M. Shabaev, and N. A. Zubova, *J. Phys. B: At. Mol. Opt. Phys.* **51**, 085001 (2018).
- [35] I. P. Grant, *Adv. Phys.* **19**, 747 (1970).
- [36] J. P. Desclaux, *Comput. Phys. Commun.* **9**, 31 (1975).
- [37] V. F. Bratzev, G. B. Deyneka, and I. I. Tupitsyn, *Bull. Acad. Sci. USSR, Phys. Ser.* **41**, 173 (1977), [*Izv. Acad. Nauk SSSR, Ser. Fiz.* **41**, 2655 (1977)].

- [38] P. Indelicato and E. Lindroth, *Phys. Rev. A* **46**, 2426 (1992).
- [39] V. A. Dzuba, V. V. Flambaum, and M. G. Kozlov, *Phys. Rev. A* **54**, 3948 (1996).
- [40] M. S. Safronova, W. R. Johnson, and A. Derevianko, *Phys. Rev. A* **60**, 4476 (1999).
- [41] I. I. Tupitsyn, V. M. Shabaev, J. R. Crespo López-Urrutia, I. Draganić, R. Soria Orts, and J. Ullrich, *Phys. Rev. A* **68**, 022511 (2003).
- [42] M. G. Kozlov, S. G. Porsev, M. S. Safronova, and I. I. Tupitsyn, *Comput. Phys. Commun.* **195**, 199 (2015).
- [43] V. A. Dzuba, J. C. Berengut, C. Harabati, and V. V. Flambaum, *Phys. Rev. A* **95**, 012503 (2017).
- [44] D. A. Glazov, A. V. Malyshev, A. V. Volotka, V. M. Shabaev, I. I. Tupitsyn, and G. Plunien, *Nucl. Instrum. Methods Phys. Res., Sect. B* **408**, 46 (2017).
- [45] T. Saue, R. Bast, A. S. P. Gomes, H. J. A. Jensen, L. Visscher, I. A. Aucar, R. Di Remigio, K. G. Dyall, E. Eliav, E. Fasshauer, T. Fleig, L. Halbert, E. D. Hedegård, B. Helmich-Paris, M. Iliáš, C. R. Jacob, S. Knecht, J. K. Laerdahl, M. L. Vidal, M. K. Nayak, M. Olejniczak, J. M. H. Olsen, M. Pernpointner, B. Senjean, A. Shee, A. Sunaga, and J. N. P. van Stralen, *J. Chem. Phys.* **152**, 204104 (2020).
- [46] V. M. Shabaev, I. I. Tupitsyn, and V. A. Yerokhin, *Phys. Rev. A* **88**, 012513 (2013).
- [47] A. V. Malyshev, D. A. Glazov, V. M. Shabaev, I. I. Tupitsyn, V. A. Yerokhin, and V. A. Zaytsev, *Phys. Rev. A* **106**, 012806 (2022).
- [48] V. M. Shabaev, I. I. Tupitsyn, and V. A. Yerokhin, *Comput. Phys. Commun.* **189**, 175 (2015); **223**, 69 (2018).
- [49] I. I. Tupitsyn, M. G. Kozlov, M. S. Safronova, V. M. Shabaev, and V. A. Dzuba, *Phys. Rev. Lett.* **117**, 253001 (2016).
- [50] L. F. Pašteka, E. Eliav, A. Borschevsky, U. Kaldor, and P. Schwerdtfeger, *Phys. Rev. Lett.* **118**, 023002 (2017).
- [51] J. Machado, C. I. Szabo, J. P. Santos, P. Amaro, M. Guerra, A. Gumberidze, Guojie Bian, J. M. Isac, and P. Indelicato, *Phys. Rev. A* **97**, 032517 (2018).
- [52] R. Si, X. L. Guo, T. Brage, C. Y. Chen, R. Hutton, and C. Froese Fischer, *Phys. Rev. A* **98**, 012504 (2018).
- [53] A. Müller, E. Lindroth, S. Bari, A. Borovik, Jr., P.-M. Hillenbrand, K. Holste, P. Indelicato, A. L. D. Kilcoyne, S. Klumpp, M. Martins, J. Viefhaus, P. Wilhelm, and S. Schippers, *Phys.*

- Rev. A **98**, 033416 (2018).
- [54] V. A. Zaytsev, I. A. Maltsev, I. I. Tupitsyn, and V. M. Shabaev, Phys. Rev. A **100**, 052504 (2019).
- [55] V. A. Yerokhin, M. Puchalski, and K. Pachucki, Phys. Rev. A **102**, 042816 (2020).
- [56] V. M. Shabaev, I. I. Tupitsyn, M. Y. Kaygorodov, Y. S. Kozhedub, A. V. Malyshev, and D. V. Mironova, Phys. Rev. A **101**, 052502 (2020).
- [57] I. I. Tupitsyn, S. V. Bezborodov, A. V. Malyshev, D. V. Mironova, and V. M. Shabaev, Opt. Spectrosc. **128**, 21 (2020).
- [58] M. Y. Kaygorodov, L. V. Skripnikov, I. I. Tupitsyn, E. Eliav, Y. S. Kozhedub, A. V. Malyshev, A. V. Oleynichenko, V. M. Shabaev, A. V. Titov, and A. V. Zaitsevskii, Phys. Rev. A **104**, 012819 (2021).
- [59] L. V. Skripnikov, J. Chem. Phys. **154**, 201101 (2021).
- [60] M. Y. Kaygorodov, D. P. Usov, E. Eliav, Y. S. Kozhedub, A. V. Malyshev, A. V. Oleynichenko, V. M. Shabaev, L. V. Skripnikov, A. V. Titov, I. I. Tupitsyn, and A. V. Zaitsevskii, Phys. Rev. A **105**, 062805 (2022).
- [61] H. Häffner, T. Beier, N. Hermanspahn, H.-J. Kluge, W. Quint, S. Stahl, J. Verdú, and G. Werth, Phys. Rev. Lett. **85**, 5308 (2000).
- [62] J. Verdú, S. Djekić, S. Stahl, T. Valenzuela, M. Vogel, G. Werth, T. Beier, H.-J. Kluge, and W. Quint, Phys. Rev. Lett. **92**, 093002 (2004).
- [63] S. Sturm, A. Wagner, B. Schabinger, J. Zatorski, Z. Harman, W. Quint, G. Werth, C. H. Keitel, and K. Blaum, Phys. Rev. Lett. **107**, 023002 (2011).
- [64] A. Wagner, S. Sturm, F. Köhler, D. A. Glazov, A. V. Volotka, G. Plunien, W. Quint, G. Werth, V. M. Shabaev, and K. Blaum, Phys. Rev. Lett. **110**, 033003 (2013).
- [65] S. Sturm, A. Wagner, M. Kretzschmar, W. Quint, G. Werth, and K. Blaum, Phys. Rev. A **87**, 030501(R) (2013).
- [66] D. A. Glazov, F. Köhler-Langes, A. V. Volotka, K. Blaum, F. Heiße, G. Plunien, W. Quint, S. Rau, V. M. Shabaev, S. Sturm, and G. Werth, Phys. Rev. Lett. **123**, 173001 (2019).
- [67] I. Arapoglou, A. Egl, M. Höcker, T. Sailer, B. Tu, A. Weigel, R. Wolf, H. Cakir, V. A. Yerokhin, N. S. Oreshkina, V. A. Agababaev, A. V. Volotka, D. V. Zinenko, D. A. Glazov, Z. Harman, C. H. Keitel, S. Sturm, and K. Blaum, Phys. Rev. Lett. **122**, 253001 (2019).

- [68] V. M. Shabaev, Phys. Rev. A **64**, 052104 (2001).
- [69] V. M. Shabaev and V. A. Yerokhin, Phys. Rev. Lett. **88**, 091801 (2002).
- [70] V. M. Shabaev, D. A. Glazov, A. V. Malyshev, and I. I. Tupitsyn, Phys. Rev. Lett. **119**, 263001 (2017).
- [71] A. V. Malyshev, V. M. Shabaev, D. A. Glazov, and I. I. Tupitsyn, JETP Lett. **106**, 765 (2017).
- [72] V. M. Shabaev, D. A. Glazov, A. V. Malyshev, and I. I. Tupitsyn, Phys. Rev. A **98**, 032512 (2018).
- [73] I. A. Aleksandrov, D. A. Glazov, A. V. Malyshev, V. M. Shabaev, and I. I. Tupitsyn, Phys. Rev. A **98**, 062521 (2018).
- [74] A. V. Malyshev, D. A. Glazov, and V. M. Shabaev, Phys. Rev. A **101**, 012513 (2020).
- [75] A. V. Malyshev, D. A. Glazov, I. A. Aleksandrov, I. I. Tupitsyn, and V. M. Shabaev, Opt. Spectrosc. **128**, 297 (2020).
- [76] D. S. Hughes and C. Eckart, Phys. Rev. **36**, 694 (1930).
- [77] V. A. Korol and M. G. Kozlov, Phys. Rev. A **76**, 022103 (2007).
- [78] Y. S. Kozhedub, A. V. Volotka, A. N. Artemyev, D. A. Glazov, G. Plunien, V. M. Shabaev, I. I. Tupitsyn, and Th. Stöhlker, Phys. Rev. A **81**, 042513 (2010).
- [79] E. Gaidamauskas, C. Nazé, P. Rynkun, G. Gaigalas, P. Jönsson, and M. Godefroid, J. Phys. B: At. Mol. Opt. Phys. **44**, 175003 (2011).
- [80] C. Nazé, S. Verdebout, P. Rynkun, G. Gaigalas, M. Godefroid, and P. Jönsson, At. Data Nucl. Data Tables **100**, 1197 (2014).
- [81] N. A. Zubova, Y. S. Kozhedub, V. M. Shabaev, I. I. Tupitsyn, A. V. Volotka, G. Plunien, C. Brandau, and Th. Stöhlker, Phys. Rev. A **90**, 062512 (2014).
- [82] C. Nazé, J. G. Li, and M. Godefroid, Phys. Rev. A **91**, 032511 (2015).
- [83] C. F. Fischer, M. Godefroid, T. Brage, P. Jönsson, and G. Gaigalas, J. Phys. B: At. Mol. Opt. Phys. **49**, 182004 (2016).
- [84] N. A. Zubova, A. V. Malyshev, I. I. Tupitsyn, V. M. Shabaev, Y. S. Kozhedub, G. Plunien, C. Brandau, and Th. Stöhlker, Phys. Rev. A **93**, 052502 (2016).
- [85] L. Filippin, J. Bieroń, G. Gaigalas, M. Godefroid, and P. Jönsson, Phys. Rev. A **96**, 042502 (2017).

- [86] I. I. Tupitsyn, N. A. Zubova, V. M. Shabaev, G. Plunien, and Th. Stöhlker, *Phys. Rev. A* **98**, 022517 (2018).
- [87] S. Gamrath, P. Palmeri, P. Quinet, S. Bouazza, and M. Godefroid, *J. Quant. Spectrosc. Radiat. Transf.* **218**, 38 (2018).
- [88] N. A. Zubova, I. S. Anisimova, M. Y. Kaygorodov, Y. S. Kozhedub, A. V. Malyshev, V. M. Shabaev, I. I. Tupitsyn, G. Plunien, C. Brandau, and T. Stöhlker, *J. Phys. B: At. Mol. Opt. Phys.* **52**, 185001 (2019).
- [89] J. Ekman, P. Jönsson, M. Godefroid, C. Nazé, G. Gaigalas, and J. Bieroń, *Comput. Phys. Commun.* **235**, 433 (2019).
- [90] N. A. Zubova, M. Y. Kaygorodov, Y. S. Kozhedub, A. V. Malyshev, R. V. Popov, I. M. Saveylyev, I. I. Tupitsyn, and V. M. Shabaev, *Opt. Spectrosc.* **128**, 1090 (2020).
- [91] R. A. Müller, V. A. Yerokhin, A. N. Artemyev, and A. Surzhykov, *Phys. Rev. A* **104**, L020802 (2021).
- [92] R. Si, S. Schiffmann, K. Wang, C. Y. Chen, and M. Godefroid, *Phys. Rev. A* **104**, 012802 (2021).
- [93] J. S. Schelfhout and J. J. McFerran, *Phys. Rev. A* **104**, 022806 (2021).
- [94] J. S. Schelfhout and J. J. McFerran, *Phys. Rev. A* **105**, 022805 (2022).
- [95] W. H. Furry, *Phys. Rev.* **81**, 115 (1951).
- [96] V. M. Shabaev, *Phys. Rep.* **356**, 119 (2002).
- [97] A. N. Artemyev, V. M. Shabaev, and V. A. Yerokhin, *J. Phys. B: At. Mol. Opt. Phys.* **28**, 5201 (1995).
- [98] V. M. Shabaev, A. N. Artemyev, T. Beier, G. Plunien, V. A. Yerokhin, and G. Soff, *Phys. Scr.* **T80**, 493 (1999).
- [99] I. A. Aleksandrov, A. A. Shchepetnov, D. A. Glazov, and V. M. Shabaev, *J. Phys. B: At. Mol. Opt. Phys.* **48**, 144004 (2015).
- [100] H. Grotch and D. R. Yennie, *Rev. Mod. Phys.* **41**, 350 (1969).
- [101] E. Borie and G. A. Rinker, *Rev. Mod. Phys.* **54**, 67 (1982).
- [102] K. Pachucki and V. A. Yerokhin, arXiv:2208.13381 [physics.atom-ph] (2022).
- [103] A. Veitia and K. Pachucki, *Phys. Rev. A* **69**, 042501 (2004).
- [104] A. V. Malyshev, I. S. Anisimova, D. V. Mironova, V. M. Shabaev, and G. Plunien, *Phys. Rev. A* **100**, 012510 (2019).

- [105] A. V. Malyshev, I. S. Anisimova, D. A. Glazov, M. Y. Kaygorodov, D. V. Mironova, G. Plunien, and V. M. Shabaev, *Phys. Rev. A* **101**, 052506 (2020).
- [106] P. J. Mohr, B. N. Taylor, and D. B. Newell, *Rev. Mod. Phys.* **84**, 1527 (2012).
- [107] J. Sapirstein and D. R. Yennie, Theory of hydrogenic bound states, in Quantum Electrodynamics, edited by T. Kinoshita, p. 560, World Scientific, Singapore, 1990.
- [108] K. Pachucki and S. G. Karshenboim, *J. Phys. B: At. Mol. Opt. Phys.* **28**, L221 (1995).
- [109] V. M. Shabaev, *J. Phys. B: At. Mol. Opt. Phys.* **26**, 4703 (1993).
- [110] M. H. Chen and K. T. Cheng, *Phys. Rev. A* **55**, 166 (1997).
- [111] K. T. Cheng, M. H. Chen, and W. R. Johnson, *Phys. Rev. A* **77**, 052504 (2008).
- [112] V. A. Yerokhin and A. Surzhykov, *Phys. Rev. A* **86**, 042507 (2012).
- [113] M. Y. Kaygorodov, Y. S. Kozhedub, I. I. Tupitsyn, A. V. Malyshev, D. A. Glazov, G. Plunien, and V. M. Shabaev, *Phys. Rev. A* **99**, 032505 (2019).
- [114] P. J. Mohr, *Ann. Phys. (N.Y.)* **88**, 26 (1974); **88**, 52 (1974).
- [115] N. J. Snyderman, *Ann. Phys. (N.Y.)* **211**, 43 (1991).
- [116] P. J. Mohr, G. Plunien, and G. Soff, *Phys. Rep.* **293**, 227 (1998).
- [117] V. A. Yerokhin and V. M. Shabaev, *Phys. Rev. A* **60**, 800 (1999).
- [118] I. Angeli and K. P. Marinova, *At. Data Nucl. Data Tables* **99**, 69 (2013).
- [119] V. A. Yerokhin and V. M. Shabaev, *J. Phys. Chem. Ref. Data* **44**, 033103 (2015).
- [120] W. R. Johnson, S. A. Blundell, and J. Sapirstein, *Phys. Rev. A* **37**, 307 (1988).
- [121] V. M. Shabaev, I. I. Tupitsyn, V. A. Yerokhin, G. Plunien, and G. Soff, *Phys. Rev. Lett.* **93**, 130405 (2004).
- [122] J. Sapirstein and K. T. Cheng, *Phys. Rev. A* **66**, 042501 (2002).
- [123] W. Kohn and L. J. Sham, *Phys. Rev.* **140**, A1133 (1965).
- [124] J. C. Slater, *Phys. Rev.* **81**, 385 (1951).
- [125] R. Latter, *Phys. Rev.* **99**, 510 (1955).
- [126] V. M. Shabaev, *Phys. Rev. A* **50**, 4521 (1994).
- [127] S. Salomonson and P. Öster, *Phys. Rev. A* **40**, 5548 (1989).